

24 ~ -100 ppm. They also have a larger quadrupole coupling constant with a larger distribution,
25 indicating greater disorder in the peraluminous glasses. It is likely that there are more Ca
26 cations present in the Cl environments in the peraluminous glasses than in the peralkaline
27 glasses despite their having the same Na/Ca ratio. In the peralkaline glasses the formation of
28 Na-Ca-Cl environments leads to a decrease in the number of network-modifying cations,
29 which causes a polymerization of the glass network. No effect on the glass polymerization
30 was observed in the peraluminous glasses. Some ^{35}Cl signal is also lost in the static spectra
31 indicating that ~ 20% of Cl for a peralkaline glass and more than ~70% for a peraluminous
32 glass must be in environments where there is a large enough electric field gradient that the
33 resulting very broad line is unobservable. These environments could be simply Na-Ca-Cl with
34 higher electric field gradients than those producing the observed ^{35}Cl signal or non-bridging
35 Cl environments like for example Al-Cl. The Cl environment in the present mixed $\text{Na}_2\text{O-CaO}$
36 aluminosilicate glasses appears to be more disordered than was to be expected from previous
37 NMR spectroscopic studies on simpler glass compositions.

38 **Keywords**

39 Chlorine, aluminosilicate, glasses, phonolites, ^{35}Cl , ^{23}Na , ^{27}Al , ^{29}Si , NMR

40 **INTRODUCTION**

41 In natural magmas chlorine (Cl) concentration usually does not exceed 1 wt%, although
42 alkali-rich magmas like phonolites can contain up to 1.2 wt% Cl (Carroll 2005; Aiuppa et al.
43 2009). Even though the abundance of Cl in natural magmatic systems is low compared to H_2O ,
44 the incorporation mechanism of Cl in silicate melts with compositions relevant to magmatic
45 systems is important as the presence of Cl can lead to the formation of brines (e.g. Sourirajan
46 and Kennedy 1962; Anderko and Pitzer 1993; Signorelli and Carroll 2000) as well as ore
47 deposits (e.g. Helgeson 1969; Webster 1997a; Candela 1997). Chlorine also influences melt

48 rheology (Dingwell and Hess 1998; Zimova and Webb 2006; Baasner et al. 2013a). Baasner
49 et al. (2013a) showed that incorporation of Cl into the system $\text{Na}_2\text{O}-\text{CaO}-\text{Al}_2\text{O}_3-\text{SiO}_2$ results
50 in contrasting behavior with 1.1 mol% (0.6 wt%) *increasing* the viscosity in peralkaline melts
51 by a factor of 10, whereas 0.6 mol% (0.3 wt%) Cl in peraluminous melts *decreases* viscosity
52 by a factor of 3.

53 Even though the incorporation mechanism of Cl in silicate melts is the key to understand the
54 behavior of Cl in magmatic systems, there are only a few studies about this topic. Stebbins
55 and Du (2002) found from ^{35}Cl magic angle spinning (MAS) nuclear magnetic resonance
56 (NMR) spectroscopy that in silicate and aluminosilicate glasses Cl is coordinated by
57 mono- and divalent cations like Na or Ba rather than by Al and Si. These authors observed
58 that in general the Cl environment is very similar in salts and glasses. For example in sodium
59 silicate and aluminosilicate glasses Cl is coordinated by less than six (as for halides) but more
60 than 4 Na cations (as in sodalite).

61 Sandland et al. (2004) concluded from ^{35}Cl MAS NMR spectroscopy that Cl in mixed
62 $\text{Na}_2\text{O}-\text{CaO}$ silicate glasses shows no strong preference for either Na or Ca. These authors also
63 found that the presence of Al or H_2O does not significantly affect the Cl environment. Evans
64 et al. (2008) investigated ^{35}Cl environment in aluminosilicate glasses containing monovalent
65 (Na, K) as well as divalent (Mg, Ca) cations with x-ray absorption near edge structure
66 (XANES) spectroscopy. They found that the salt-like Cl environments in magmatic melts are
67 dominated by Ca and Mg and that alkali content, redox conditions and water only play a
68 subsidiary role.

69 There are only two NMR studies of ^{35}Cl in silicate glasses, probably because spectra of ^{35}Cl
70 in glasses are much more difficult to measure and interpret than that of other nuclei such as
71 ^{19}F or ^{23}Na . The solubility of Cl in (alumino)silicate glasses is usually lower than 2 wt% for
72 0 - 200 MPa (Webster 1997b; Carroll 2005; Tanimoto and Rehren 2008) and, as ^{35}Cl is a

73 quadrupole nucleus with a spin of $I = 3/2$, a large quadrupole moment and a low Larmor
74 frequency, its line shape, even at high magnetic fields under MAS conditions, is severely
75 influenced by second order quadrupole broadening (e.g. Sandland et al. 2004). Literature
76 reports a large variation of quadrupole coupling constants (C_q) for ^{35}Cl ranging from a few
77 MHz up to 80 MHz (e.g. Johnson et al. 1969; Lucken 1969; Sandland et al. 2004; Gervais et
78 al. 2005). Note, that linewidth is proportional to C_q^2 (e.g. Freude and Haase 1993). ^{35}Cl also
79 has a large (> 1000 ppm) chemical shift range (Johnson et al. 1969; Sandland et al. 2004)
80 further broadening the peak in disordered systems, thus the acquisition of ^{35}Cl spectra of
81 glasses with an acceptable signal to noise ratio, even at magnetic fields of 14.1 T and higher,
82 takes more than a day.

83 To date the Cl environment in mixed Na_2O - CaO aluminosilicate glasses as a function of the
84 Al concentration has not been studied. In this work we investigate the incorporation
85 mechanism of 0.6 - 1.9 mol% (0.3 - 1 wt%) Cl in peralkaline ($[\text{Na}_2\text{O}+\text{CaO}] > \text{Al}_2\text{O}_3$) and
86 peraluminous ($[\text{Na}_2\text{O}+\text{CaO}] < \text{Al}_2\text{O}_3$) Na_2O - CaO aluminosilicate glasses with about 66 mol%
87 SiO_2 , which are a first approximation for phonolitic melts, using ^{35}Cl , ^{27}Al , ^{23}Na and ^{29}Si
88 MAS NMR spectroscopy. The general differences between halogen-free peralkaline and
89 peraluminous spectra and their relation to structure have been discussed previously by
90 Baasner et al. (2014). The focus of this paper will be on the incorporation mechanism of Cl.

91

92

METHODS

93 Starting Materials

94 Peralkaline (NACS) and peraluminous (ANCS) Na_2O - CaO aluminosilicate glasses containing
95 Cl alone or combined with F were synthesized from powdered oxides, carbonates, halides and
96 ammonium halides. In addition, one Cl-bearing sodium silicate glass (NS) was synthesized.

4

97 The powder mixtures were decarbonated for 12 h at 1173 K at 1 atm and then melted at
98 1473 - 1923 K for several hours in a Pt crucible in an 1 atm furnace. The glasses were crushed
99 and remelted several times to achieve chemical homogenization. The sample ANCS 1.2Cl
100 was synthesized in a piston cylinder apparatus at 1923 K and 500 MPa for 3 h in a Pt₉₀Rh₁₀
101 capsule (detailed description in Baasner et al. 2013b). In order to achieve a higher Cl content
102 than in the other peraluminous samples produced at 1 atm, we synthesized this sample under
103 pressure to reduce the vaporization of Cl before it dissolves in the melt. Some of the
104 samples were doped with < 0.1 wt% CoO to enhance the spin lattice relaxation.

105 The compositions of the glasses were determined using a JEOL JXA-8900RL electron
106 microprobe with eight to ten measurements per sample using a 15 kV and 15 nA beam
107 defocused to 30 μm. Table 1a, b presents the compositions of the glasses in mol% oxides and
108 in atom% (at%). The notation in at% takes into account that there is one O²⁻ less for two Cl⁻ or
109 F⁻. Table 1a also shows the (Na₂O+CaO)/(Na₂O+CaO+Al₂O₃) ratio, which is referred as R
110 value (e.g. Thompson and Stebbins 2011) or the gamma value (e.g. Toplis et al. 1997; Webb
111 et al. 2007). Peralkaline glasses have an R > 0.5 indicating that there are enough Na and Ca
112 cations to charge balance Al-tetrahedra (Al coordinated by four oxygens) and that the
113 remaining Na and Ca cations exist as network-modifiers, which create mostly non-bridging
114 oxygens (NBO) at Si-tetrahedra (Si coordinated by four oxygens), which can be seen from
115 NMR spectroscopy (e.g. Allwardt et al. 2003; Lee 2004; Lee and Stebbins 2009).
116 Peraluminous glasses have an R < 0.5 indicating that there are not enough Na and Ca cations
117 to charge-balance all Al-tetrahedra, which leads to the formation of higher-coordinated Al
118 (Schmücker et al. 1997; Kohn et al. 1991) or triclusters (Toplis et al. 1997) and that there are
119 (nearly) no network-modifying cations that create NBO's (Thompson and Stebbins 2011).

120 The Ca/[Ca+Na] ratio (Table 1b) in the peralkaline and the peraluminous samples is almost
121 the same (~ 0.15 and ~ 0.17) although it is slightly higher for peraluminous glasses as they

122 were produced in the 1 atm furnace at significantly higher temperatures than the peralkaline
123 glasses, which caused some Na volatilization and a relative enrichment in Ca of the melt. The
124 Cl concentration of the samples NS 2.2Cl and NACS 1.1Cl was confirmed with laser-ablation
125 inductive coupled plasma mass spectrometry (LA-ICPMS).

126

127 **NMR measurements**

128 All NMR measurements in this study were performed at University of Warwick except for the
129 very high field ^{35}Cl MAS data, which were collected at 81.599 MHz on an 830 MHz Bruker
130 DRX (19.6 T) spectrometer at the National High Magnetic Field Laboratory, Tallahassee. ^{35}Cl
131 MAS spectra were also collected at 58.726 MHz on a 600 MHz Bruker Avance II+ (14.1 T)
132 or at 59.010 MHz on a 600 MHz Varian (14.1 T) spectrometer. At 14.1 T a 3.2 mm rotor with
133 a spinning speed of 20 kHz was used and the spectra were collected using an echo sequence
134 with pulse lengths of 1.75 (a solids 90°) and 3.5 μs (a solids 180°), an inter-pulse spacing of
135 one rotor cycle (sample NACS 1.1Cl was also run with a 4 rotor cycle inter-pulse spacing for
136 comparison), a recycle delay of 0.1 s and 36,000 - 2,300,000 acquisitions. Note, in our
137 samples we are in the large C_q limit for ^{35}Cl , i.e. only the $\frac{1}{2} \rightarrow -\frac{1}{2}$ transition is irradiated ($C_q >$
138 ~ 1.5 MHz), thus the pulse lengths required are $1/(I+1/2)$ of those for a liquid or sample with
139 near zero C_q (e.g. NaCl). The inter-pulse spacing and the recycle delay were carefully tested
140 to avoid saturation or any other distortion of the signal. In addition, static spectra of the
141 samples NS 2.2Cl, NACS 1.1Cl, ANCS 1.0F 0.9Cl were collected at 14.1 T in a 10 mm static
142 probe with an echo spacing of 250 μs , pulse lengths of 3.25 and 6.5 μs , a recycle delay of
143 0.1 s and 730,000 - 2,300,000 acquisitions. Different recycle delays were tested for NACS
144 1.1Cl and the signal intensity was the same within the noise level from 0.1s upwards. The
145 spectra at 19.6 T were collected in a 1.8 mm rotor with a spinning speed of 30 kHz. The
146 spectra were measured using an echo sequence with pulse lengths of 1.85 (a solids 90°) and

6

147 3.7 μ s (a solids 180°), an inter-pulse delay of 4 rotor cycles, a recycle delay of 0.1 s and
148 70,000 - 4,800,000 acquisitions (total time 6 days). Solid NaCl was used as reference and was
149 set to -46 ppm relative to 1 M aqueous NaCl solution.

150 ²³Na MAS spectra were collected at 132.286 MHz on a 500 MHz Bruker Avance III (11.7 T)
151 spectrometer. The samples were measured in a 2.5 mm rotor with a spinning speed of 26 kHz,
152 a pulse length of 1.5 μ s (a solids 90°), a recycle delay of 1 s and 60 - 660 acquisitions. Solid
153 NaCl was used as reference that was set to -7 ppm relative to 1 M aqueous NaCl solution.

154 ²⁷Al MAS spectra were collected at 130.301 MHz on a 500 MHz Bruker Avance III (11.7 T)
155 and at 221.550 MHz on an 850 MHz Bruker Avance III (20 T) spectrometer. The samples at
156 11.7 T were measured in a 2.5 mm rotor with a spinning speed of 26 kHz, a pulse length of
157 0.75 μ s, a recycle delay of 1 s and 1,600 - 16,000 acquisitions. The samples at 20 T were
158 measured in a 3.2 mm rotor with a spinning speed of 20 kHz, a pulse length of 0.8 μ s, a
159 recycle delay of 2 s and 84 acquisitions. The peak of six-coordinated Al in yttrium aluminum
160 garnet (YAG) was used as reference and was set to 0.7 ppm relative to 1 M aqueous AlCl₃
161 solution. In all experiments the pulse length corresponds to an angle less than a solids 90°.

162 ²⁹Si MAS spectra were collected at 59.615 MHz on a 300 MHz Varian Infinity Plus (7 T)
163 spectrometer. The samples were measured in a 7 mm rotor with a spinning speed of 4 kHz, a
164 pulse length of 3.5 μ s (45°), a recycle delay of 30 - 60 s and 172 - 2,544 acquisitions (spectra
165 for the samples ANCS 0.6Cl and ANCS 1.2Cl were not measured due to failure of the
166 spectrometer). Kaolinite was used as reference and was set to -91.5 ppm relative to
167 tetramethylsilane (TMS, Si(CH₃)₄).

168

169

RESULTS

170 **³⁵Cl MAS NMR**

171 Figures 1 and 2 show the ³⁵Cl MAS NMR spectra of the Cl-bearing samples at 14.1 and
172 19.6 T. The spectrum of the Na₂O-SiO₂ glass has a quadrupole tail on the right hand side. In
173 contrast, the lines of the peralkaline and peraluminous glasses are broader, lower in intensity,
174 and approximately Gaussian with only a small quadrupole tail visible on the right hand side
175 for some samples. The term “quadrupole tail” describes the asymmetric intensity distribution
176 on the lower frequency flank of the peak, which is a common feature in NMR spectra of
177 quadrupole nuclei (e.g. ³⁵Cl, ²³Na or ²⁷Al) in disordered solids when the nuclei exist in
178 environments with a symmetry less than a perfect sphere or octahedron (e.g. Kirkpatrick
179 1988; Stebbins 1995). The signal to noise ratio of the ³⁵Cl spectra (Figs. 1 and 2) decreases
180 from the sodium silicate glass to the peralkaline glasses to the peraluminous glasses, although
181 the peraluminous samples were collected with the higher number of acquisitions. Compared
182 to the sodium silicate glass and normalized to same amount of Cl atoms and number of
183 acquisitions only ~ 60% of the ³⁵Cl MAS NMR signal was observed for the peralkaline
184 glasses and only ~ 25% for the peraluminous glasses. The effect of different sample densities
185 and rotor packing on the signal intensities is less than 10%. However the widths of the lines
186 for peralkaline and peraluminous glasses are much broader than those of the sodium silicate
187 glass, ~ 10 kHz and > ~ 15 kHz respectively. This suggests that a significant amount of the Cl
188 exists in environments with a large enough electric field gradient that the intensity of the
189 central band is reduced because significant intensity appears in the sidebands and/or the
190 linewidth is too large to be narrowed by the MAS experiment (Massiot et al. 1990).

191 Figure 3 shows the spectra of the peralkaline glass NACS 1.9Cl and the peraluminous glass
192 ANCS 1.2Cl at 14.1 T normalized to the same number of acquisitions and the same number of
193 Cl atoms. For ANCS 1.2Cl compared to NACS 1.9Cl only about half of the ³⁵Cl signal was
194 obtained. Fig. 3 also shows that there is a small broad, un-narrowed background underneath

195 the ^{35}Cl peak, which is similar for both spectra. The static NMR spectrum of the peralkaline
196 sample NACS 1.1Cl (Fig. 4) extends over ~ 94 kHz (600 to -1000 ppm) and $\sim 80\%$ of the
197 ^{35}Cl signal was detected compared with the sodium silicate glass (NS 2.2Cl). The static NMR
198 spectrum of the peraluminous glass ANCS 1.0F 0.9Cl shows an even broader ^{35}Cl peak that
199 extends over ~ 130 kHz (900 to -1300 ppm) with less than 30% of the ^{35}Cl signal compared to
200 the sodium silicate glass (Fig. A in the supplementary data). In general the static line shapes
201 are consistent with the parameters obtained from MAS NMR spectroscopy in Tables 2 - 4.
202 Thus the remaining Cl must be in environments with a large electric field gradient that results
203 in an extremely broad and unobservable line.

204 Table 2 gives the peak maxima, the centers of gravity and the full width half maxima *FWHM*
205 of the ^{35}Cl MAS NMR spectra. The centers of gravity of the peralkaline glasses and the
206 sodium silicate glass are similar with ~ -155 ppm at 14.1 T and ~ -130 ppm at 19.6 T, while the
207 centers of gravity of the peraluminous glasses are shifted to higher ppm values of ~ -140 ppm
208 at 14.1 T and ~ -115 ppm 19.6 T. In case of the spectra at 14.1 T, the spinning sidebands are
209 not completely separated from the central band, which contributes to an error of ± 5 ppm for
210 the centers of gravity. The *FWHM* increases by a factor two or more at both fields from
211 sodium silicate to peraluminous glasses.

212 Figure 5 shows an overlay of the ^{35}Cl MAS NMR spectra of peralkaline and peraluminous
213 glasses at 14.1 T and 19.6 T normalized to same peak height. The increased width together
214 with a shift of the ^{35}Cl resonance to higher ppm values in the peraluminous glass compared to
215 the peralkaline glass can be clearly seen from both overlays.

216 Figure 6 shows the center of gravity δ_{cg} [ppm] as function of the inverse squared Larmor
217 frequency ν_0^{-2} [MHz $^{-2}$] for some of the Cl-bearing samples. Linear equations were used to fit
218 the data. The ordinates of the linear equations give the isotropic chemical shift δ_{iso} [ppm]
219 (Table 3). A mean quadrupole coupling constant C_q [MHz] (Table 3) can be calculated from

220 the slope of Eq. 1 (after e.g. Freude and Haase 1993; Schmidt et al. 2000a) using the
221 asymmetry parameter $\eta = 0.7$ (Stebbins and Du 2002)

$$222 \quad \delta_{cg} = \delta_{iso} - \frac{1}{40} \cdot \frac{C_q^2 \cdot (1 + \eta^2 / 3)}{\nu_0^2}. \quad (1)$$

223 For the peralkaline glasses the spectra of the samples NACS 1.1Cl and NACS 1.9Cl were
224 used for the plot in Fig. 6. For the peraluminous glasses the spectrum of ANCS 0.6Cl at
225 19.6 T and the spectrum of ANCS 1.2Cl at 14.1 T was used as the spectrum of ANCS 0.6Cl at
226 14.1 T had a very poor signal to noise ratio. The higher concentration of Cl in ANCS 1.2Cl
227 compared to ANCS 0.6Cl is not expected to have a significant influence on the results (e.g.
228 Stebbins and Du 2002; Sandland et al. 2004) as the concentration of Cl is low. The center of
229 gravity vs. inverse squared Larmor frequency plots for the other samples containing both, Cl
230 and F, are given in Figs. B and C in the supplementary data. Having data at only two fields,
231 along with the errors of the centers of gravity (± 5 ppm) and the unknown real value of the
232 asymmetry parameter η , results in significant uncertainty in these parameters (estimated as \sim
233 ± 16 ppm for δ_{iso} and $\sim \pm 0.3$ MHz for C_q) and the real errors might be higher. Therefore, we
234 also provide later in the text an alternate evaluation method using the program Quadfit (Kemp
235 et al. 2009).

236 An estimate of the width due to the quadrupole effect W_q and the width due to the chemical
237 shift distribution W_{csd} (Table 3) can be calculated after Schmidt et al. (2000a, b)

$$238 \quad FWHM_1^2 = W_q^2 + W_{csd}^2 \quad (2)$$

239 and

$$240 \quad FWHM_2^2 = (B_1 / B_2)^2 W_q^2 + (B_2 / B_1)^2 W_{csd}^2. \quad (3)$$

241 with $FWHM_1$ and $FWHM_2$ [Hz] being the full width half maxima of two spectra measured at a
242 lower magnetic field B_1 [T] and a higher magnetic field B_2 [T]. Because of the low signal to
243 noise ratio W_q and W_{csd} of the samples ANCS 0.6Cl and ANCS 1.0F 0.9Cl are not presented.

244 The sodium silicate glass and the peralkaline glass have, within error (± 16 ppm), the same
245 isotropic chemical shift of ~ -100 ppm, while the peraluminous glasses have a higher
246 chemical shift of ~ -75 ppm. The mean C_q 's of the samples range from 2.3 - 3.1 MHz. The
247 presence of F only has a minor influence, comparable with the error, on the chemical shift and
248 C_q . The chemical shift dispersion, W_{csd} , for the sodium silicate glass is ~ 60 ppm, smaller than
249 that of the peralkaline glasses, $\sim 80 - 90$ ppm (Table 3). The values for W_q are only 50% larger
250 than those of W_{csd} at 14.1 T for both glasses. At 19.6 T W_{csd} is the dominant contribution to
251 the linewidth, even though second-order quadrupole broadening is still affecting the signal,
252 which is consistent with the relatively small C_q for ^{35}Cl observed here.

253 An alternate way of describing the effect of significant distributions in the parameters, if data
254 at more than one field are available, is to use programs such as Quadfit to simulate the spectra
255 (Kemp et al. 2009). Quadfit not only uses the parameter δ_{iso} , a mean \bar{C}_q , W_{csd} and a mean $\bar{\eta}$
256 for simulation, but also allows a distribution of C_q ($\Delta\bar{C}_q$) and η ($\Delta\bar{\eta}$). Using Quadfit to fit
257 the spectra with a single quadrupole line, worked well for the NS glass (Fig. D in the
258 supplementary data) but was not entirely successful for the peraluminous and peralkaline
259 glasses. Figure 7 shows, as an example, the spectrum of NACS 1.1Cl at 14.1 T and 19.6 T
260 simulated with Quadfit. There is some additional intensity ($\sim 10 - 20\%$) on the high frequency
261 flank of the peralkaline and peraluminous spectra that could not be simulated. The presence of
262 this feature in spectra of different samples from different magnetic fields suggests that there
263 might be more than one type of Cl environment, although the signal to noise ratio of our
264 spectra implies some uncertainty regarding this point. The parameters obtained from peak
265 fitting of all spectra except ANCS 0.6Cl at 14.1 T (because of too low signal to noise) are

266 given in Table 4. The parameters suggest that for the sodium silicate, peralkaline and
267 peraluminous glasses the mean chemical shifts, δ_{iso} are -80 ppm, -74 to -79 ppm, and -30
268 to -58 ppm respectively, whilst the distribution in chemical shifts W_{csd} increases from 37 ppm
269 to ~ 75 ppm and to ~ 125 ppm. The mean quadrupole coupling constant \bar{C}_q also increases
270 from ~ 3.5 MHz in the sodium silicate and peralkaline glasses to ~ 4.2 MHz for the
271 peraluminous glasses. For all glasses the distribution of the quadrupole coupling constant is
272 large, $\Delta\bar{C}_q \geq 2.1 - 3.0$ MHz, with the peraluminous samples having the highest values. The
273 mean asymmetry parameter $\bar{\eta}$ ranges from 0.5 to 0.8 with a distribution $\Delta\bar{\eta} \geq 0.2$. In
274 summary, the values for the isotropic chemical shifts simulated with Quadfit are ~ 20 - 30 ppm
275 more positive and the quadrupole coupling constants ~ 1 MHz larger than those obtained
276 using the method of Schmidt et al. (2000a, b), however both methods show the same trends:
277 The peralkaline glasses have similar chemical shifts to the sodium silicate glass with the
278 peraluminous glasses having a ~ 25 - 40 ppm higher chemical shift. Both the chemical shift
279 dispersion and the distribution in quadrupole coupling constants increase markedly from
280 sodium silicate to peralkaline to peraluminous glass.

281

282 ²³Na MAS NMR

283 Figure 8 shows ²³Na MAS NMR spectra at 11.7 T. The peak shape is nearly Gaussian. The
284 peak maxima, centers of gravity and the *FWHM* are given in Table 5. The peak parameters
285 and the spectra of the halogen-free samples NACS and ANCS were taken from Baasner et al.
286 (2014). The peak maximum of the halogen-free peralkaline glass has a higher shift, -17.0 ppm,
287 and the *FWHM* is broader, 25.7 ppm, than that of the halogen-free peraluminous
288 glass, -20.7 ppm and 20.7 ppm respectively. In the peralkaline as well as in the peraluminous
289 glasses containing the highest Cl concentration the presence of Cl causes a small positive shift

290 in the peak maxima of up to 2 ppm while the centers of gravity and the *FWHM* remain
291 constant.

292

293 ²⁷Al MAS NMR

294 The peak maxima, centers of gravity and the *FWHM* of the ²⁷Al MAS NMR spectra are given
295 in Table 6. The peak parameters and the spectra of the halogen-free sample NACS and ANCS
296 were taken from Baasner et al. (2014) including the calculation of δ_{iso} and C_q after Schmidt et
297 al. (2000a).

298 Figure 9 shows ²⁷Al MAS NMR spectra at 11.7 T of the halogen-free peralkaline sample
299 NACS and the Cl-bearing glass NACS 1.9Cl. The peaks have an obvious quadrupole tail on
300 the right hand side. All Al is four-coordinated (^{IV}Al) with a peak maximum at ~ 55 ppm, no
301 higher-coordinated Al (^VAl or ^{VI}Al) is observed and the spectrum of Cl-bearing glass NACS
302 1.9Cl is virtually identical to that of the halogen-free glass NACS.

303 Figure 10 shows ²⁷Al MAS NMR spectra at 20 T of the halogen-free peraluminous sample
304 ANCS and the Cl-bearing glass ANCS 1.2Cl. Despite the high field a quadrupole tail on the
305 right hand of the peaks is still visible. As found earlier for the halogen-free glass (Baasner et
306 al. 2014) most Al is ^{IV}Al with a peak maximum at ~ 57 ppm and a small (5 - 6% of the total
307 Al) fraction of ^VAl around 30 ppm in both spectra. A subtraction of the spectrum of ANCS
308 from ANCS 1.2Cl shows that the spectra are very similar although the amount of ^VAl might
309 be slightly higher (< 1%) in the Cl-bearing glass than in the Cl-free glass.

310

311 ²⁹Si MAS NMR

312 Figure 11 shows ^{29}Si MAS NMR spectra at 7 T of the halogen-free and Cl-bearing peralkaline
313 and peraluminous glasses. The lines have a Gaussian shape and the peak maxima, centers of
314 gravity and *FWHM* are given in Table 7. The peak parameters and the spectra of the
315 halogen-free samples NACS and ANCS were taken from Baasner et al. (2014). The
316 halogen-free peraluminous sample ANCS has a lower chemical shift, -100.4 ppm, than the
317 halogen-free peralkaline sample NACS, -96.3 ppm. The ^{29}Si peak in the peraluminous glasses
318 is unaffected by the presence of Cl (and F), while in the peralkaline glasses Cl causes a small
319 shift in the peak maximum of -0.9 ppm and -1.7 ppm in the centre of gravity. The ^{29}Si peaks
320 in the spectra of NACS 1.1Cl and NACS 1.0F 0.9Cl are within error the same.

321

322

DISCUSSION

323 The values for mean isotropic chemical shift and quadrupole parameters derived from the
324 methods of Schmidt et al. (2000a, b) and the program Quadfit (QF) show similar trends
325 although the values are somewhat different. However the methods used to determine δ_{iso} , C_q ,
326 W_{csd} and W_q for the ^{35}Cl spectra (Schmidt et al. 2000a, b) (Fig. 6) are intended for peaks that
327 were produced by a single environment without a large dispersion in C_q , although the ^{35}Cl
328 lineshape for the peralkaline and peraluminous glasses indicates that this is not the case.

329 Sandland et al. (2004) suggested that in mixed Na_2O - CaO silicate glasses Cl exists in
330 environments surrounded by either Ca or Na cations as well as in mixed cation environments.
331 However the spectra of the peralkaline and peraluminous glasses are not well enough
332 constrained to allow a meaningful fit to multiple peaks even though there is some evidence
333 that a one site simulation with Quadfit is insufficient (see e.g. Fig.7). Stebbins and Du (2002)
334 and Sandland et al. (2004) found that calcium (alumino)silicate glasses have a ~ 150 ppm
335 higher ^{35}Cl isotropic chemical shift (52 to 102 ppm) than sodium (alumino)silicate glasses

336 (-65 to -89 ppm) and that mixed Na₂O-CaO silicate glasses have an intermediate shift. No
337 data are available for mixed Na₂O-CaO aluminosilicate glasses. The present peralkaline
338 mixed Na₂O-CaO aluminosilicate glasses have a similar ³⁵Cl chemical shift to sodium silicate
339 glass, ~ -100 ppm (~ -76 ppm, QF) (Figs. 1, 2 and 4), suggesting that the ³⁵Cl sites are
340 dominated by Na and that the Cl environments are very similar in both glass types, but with
341 more disorder in the peralkaline glass. This was expected as in the peralkaline Na₂O-CaO
342 aluminosilicate glasses with a Ca/[Ca+Na] ratio of 0.18 the Na concentration is much higher
343 than the Ca concentration. The *FWHM* and *W_{csd}* of the ³⁵Cl MAS NMR signal is significantly
344 broader in the peralkaline Na₂O-CaO aluminosilicate glasses than in the sodium silicate glass
345 indicating a significantly larger chemical shift distribution, which could be either related to
346 the incorporation of Ca cations in the Cl environment or due to the presence of Al. The latter
347 is unlikely as the comparison of Al-bearing and Al-free glasses in previous studies showed
348 that Al has no strong influence on the ³⁵Cl environment (Stebbins and Du 2002; Sandland et
349 al. 2004). Sandland et al. (2004) observed no preference of Cl for Ca or Na cations in mixed
350 Na₂O-CaO silicate glasses. However, the ³⁵Cl MAS NMR resonance of the peraluminous
351 mixed Na₂O-CaO aluminosilicate glasses is shifted by ~ +25 ppm (~ +40 ppm QF) (Figs. 1, 2,
352 3 and 5) and the chemical shift distribution is ~ 50% larger than for the peralkaline glasses. In
353 analogy to the data of Stebbins and Du (2002) and Sandland et al. (2004) this shift may
354 indicate that more Ca cations relative to Na cations are incorporated in the Cl sites even
355 though the samples have the same Ca/[Ca+Na] ratio. This suggests that Cl has a slight
356 preference for Na cations compared to Ca cations in peralkaline samples. In the peraluminous
357 glasses, where most Na and Ca cations are assumed to charge-balance Al-tetrahedra, the Na
358 and Ca cations cannot arrange as freely as in the peralkaline glasses and presumably therefore,
359 more Ca is incorporated in the Cl environment.

360 The comparatively small ³⁵Cl *C_q* values of 2 - 4 MHz (Tables 3 and 4) for the peralkaline,
361 peraluminous and sodium silicate glasses are consistent with previous studies and indicate

362 that the Na-Ca-Cl environments are relatively symmetric (Stebbins and Du 2002; Sandland et
363 al. 2004). The 2 ppm positive shift in the ^{23}Na spectra due to the presence of Cl in the
364 peralkaline as well as in the peraluminous glasses (Fig. 8) is consistent with the formation of
365 salt-like structural units similar to that in NaCl (Stebbins and Du 2002), which would lie with
366 a shift of 0 ppm in the high frequency flank of the ^{23}Na resonance of the glasses. Overall,
367 except for the higher amount of Ca that is incorporated in the Na-Ca-Cl environments in the
368 peraluminous glasses compared to the peralkaline glasses, the environments seem to be
369 similar. A similarity was quite unexpected as Stebbins and Du 2002 and Sandland et al. 2004
370 proposed that Cl bonds to network-modifying cations, which do not exist in significant
371 quantities in peraluminous glasses (Stebbins and Xu, 1997; Thompson and Stebbins, 2011).
372 However, the ^{35}Cl signal shows that a significant fraction of Cl atoms in the peraluminous
373 glasses are in relatively symmetric Na-Ca-Cl environments. There are two possible
374 explanations for this: first, Cl in peraluminous glasses could occupy interstitial positions in
375 the glass network between charge-balancing cations at Al-tetrahedra. If one assumes that the
376 charge-balancing Na and Ca cations are randomly distributed, this incorporation mechanism
377 would explain the higher amount of Ca cations in the Cl environment although it might have a
378 preference for Na cations like in the peralkaline glasses. Second, as recently shown by
379 Thompson and Stebbins (2011) with ^{17}O NMR, peraluminous glasses are not necessarily
380 completely free of non-bridging oxygens, which would allow a small quantity of
381 network-modifying cations to exist and to build Na-Ca-Cl environments. However, a
382 quantification of the non-bridging oxygens is not possible since no ^{17}O NMR data is available
383 for our composition.

384 In the peralkaline glasses the ^{29}Si peak of the Cl-bearing glasses NACS 1.1Cl and NACS 1.0F
385 1.0Cl are shifted to lower frequencies compared to the halogen-free glass NACS (Fig. 11),
386 which may indicate that Cl causes further polymerization of the glass-network (Engelhardt
387 and Michel 1987). Si-Cl environments could not be responsible for the shift, because the

388 isotropic chemical shift for ^{29}Si in SiCl_4 is -18.5 ppm (Marsmann et al. 1983), which would
389 shift the signal to higher frequencies. This suggests that in peralkaline glasses the formation
390 of Na-Ca-Cl environments reduces the number of network-modifying Na and Ca cations and,
391 therefore, reduces the number of non-bridging oxygens, which leads to further polymerization
392 of the glass network. A further polymerization of the silicate-network would cause an increase
393 in viscosity, which was indeed observed by Baasner et al. (2013a) for peralkaline samples
394 with the same composition. An Al-Cl interaction, which could reduce the amount of Al-Si
395 bonds and thus could cause a negative shift of the ^{29}Si signal, seems unlikely to be prevalent
396 in case of the peralkaline samples, as such an interaction would cause a decrease in viscosity
397 by transforming charge balancing cations into network modifiers. In contrast, the ^{29}Si
398 spectrum of the peraluminous glass ANCS 1.0F 0.9Cl shows no difference due to the
399 presence of F and Cl compared to the spectrum of the halogen-free glass ANCS (Fig. 11).
400 Fluorine was found to cause a negative chemical shift of the ^{29}Si peak in peraluminous glasses
401 of -1 ppm for a concentration of 9.7 mol% F (Baasner et al. 2014), which is ten times as much
402 F as in ANCS 1.0F 0.9Cl. Thus, if Cl would have caused a shift in the spectrum of ANCS
403 1.0F 0.9Cl compared to ANCS, it would not be masked by an effect of F. In the fully
404 polymerized peraluminous glasses all Na and Ca cations are charge-balancing Al and nearly
405 all Si-tetrahedra are fully connected with bridging oxygens to other Si- or Al-tetrahedra (e.g.
406 Lee 2004; Lee and Stebbins 2009; Thompson and Stebbins 2011). Therefore, Cl in
407 peraluminous glasses should not have an influence on the Si environment by bonding to Na or
408 Ca as in the peralkaline glasses, since the Si-tetrahedra are already fully polymerized.

409 Cl as a monovalent anion could compensate one positive charge of a charge-balancing cation
410 by bonding to Na and Ca and, therefore, could create $^{\text{V}}\text{Al}$ in peraluminous glasses (e.g.
411 Thompson and Stebbins 2011). We only observed a slight increase of, at most, 1% in $^{\text{V}}\text{Al}$ in
412 the ^{27}Al spectrum of ANCS 1.2Cl compared to that of ANCS, although this increase could be
413 within the error (Fig. 10). However, a strong increase in $^{\text{V}}\text{Al}$ due to Cl in the peraluminous

414 glasses was not expected as the Cl concentration is small, 1.2 mol%, and less than 50% of the
415 Cl exist in Na-Ca-Cl environments. Even if one assumes that one Cl anion could create one
416 ^VAl , one would expect only an increase of 2% in ^VAl . Furthermore a recent study by
417 Thompson and Stebbins (2011) showed that an excess of 1 mol% Al compared to
418 charge-balancing cations in peraluminous glasses is likely to result in the formation of only
419 0.25 mol% ^VAl .

420 Compared to the sodium silicate glass only ~ 60% of the ^{35}Cl MAS NMR signal for the
421 peralkaline glasses and ~ 25% for the peraluminous glasses normalized to the same number of
422 acquisitions and molar concentration of Cl (Fig. 3) is observed. The values for C_q and the
423 distribution in C_q are large enough to explain a significant proportion of the missing signal in
424 terms of not spinning fast enough (Massiot et al. 1990; Table 4). However even in the static
425 NMR spectrum (Fig. 4), which extends over ~ 94 kHz only ~ 80% of the ^{35}Cl signal was
426 observed for the peralkaline glass NACS 1.1Cl and less than ~ 30% for the peraluminous
427 glass (Fig. A in the supplementary data) compared to the sodium silicate glass NS 2.2Cl. The
428 simplest explanation for the missing signal would be, that the ^{35}Cl concentration in the
429 samples or the amount of the sample in the rotor is less than expected. However, we
430 confirmed the Cl concentration measured with the electron microprobe with LA-ICPMS. A
431 different filling of the rotors could cause only a difference in sample mass of ~ 5 to 10%
432 (Baasner et al. 2013a; Baasner et al. 2013b). There are several possibilities that could produce
433 an electric field gradient large enough to make the signal unobservable by NMR spectroscopy,
434 e.g. a higher asymmetry and/or a higher diversity within the nearest neighbors of some of the
435 Cl environments. Three structural configurations of Cl are conceivable that explain the
436 missing signal: First, the Cl exists in asymmetric interstitial positions between Na and Ca
437 cations, presumably charge-balancing cations that remain in their charge-balancing role and
438 are, therefore, not as free to arrange as the network-modifying cations. Second, Al or Si
439 cations are involved in the Cl environment like in AlCl_3 or SiCl_4 , which both have a high

440 quadrupole coupling constant of more than 9 MHz (Sandland et al. 2004; Johnson et al. 1969)
441 and, therefore, would not be observed. Third, Cl could, instead of replacing all oxygens
442 around Al or Si, replace some or single bridging oxygens between Al- and Si-tetrahedra and
443 then be additionally surrounded by other cations like Ca or Na, as was observed for F in
444 aluminosilicate glasses (e.g. Schaller et al. 1992; Stebbins et al. 2000; Stebbins and Zeng
445 2000; Zeng and Stebbins 2000; Kiczenski and Stebbins 2002; Mysen et al. 2004; Stamboulis
446 et al. 2005; Karpukhina et al. 2008; Baasner et al. 2014). However, it is unknown if the
447 quadrupole coupling constant would be as high as for AlCl or SiCl₄. We observed no
448 significant influence of Cl on the ²⁷Al or ²⁹Si environments in the peraluminous glasses
449 (Figs. 10 and 11) that could show evidence for the second and third possibility. However, the
450 amount of Cl is too small compared to that of Al and Si to definitely exclude Al-Cl or Si-Cl
451 environments. Some signal is also missing in case of the peralkaline samples, which is also an
452 argument against the existence of significant amounts of Al-Cl or Si-Cl environments. These
453 environments would cause a depolymerization of the silicate network and a decrease in
454 viscosity. However, Baasner et al. (2013a) found for peralkaline samples with the same
455 composition that the addition of Cl increases viscosity and this increase appears to be too
456 strong to leave space for significant amounts of Cl environments that cause a decrease in
457 viscosity. Though, we cannot exclude minor fractions of Al-Cl or Si-Cl environments. We
458 think that the first explanation for the missing signal is the most likely, as our Quadfit
459 simulations indicate (Table 4) that the quadrupole distribution of the Na-Ca-Cl environments
460 is large, 2.1 - 3 MHz, in the aluminosilicate glasses. Since the simulation does not take
461 spinning speed into account, it is likely that the quadrupole distribution is, in some cases, even
462 larger than estimated. In this case the long quadrupole tail caused by the distribution, which is
463 difficult to detect, would be underestimated. The observation of a missing ³⁵Cl signal in
464 aluminosilicate glasses was not made in the previous studies of Stebbins and Du (2002) or of
465 Sandland et al. (2004) who observed at least 90% of the ³⁵Cl signal in their aluminosilicate

466 glasses compared to silicate glasses. They investigated pure subaluminous Na₂O and
467 peralkaline to subaluminous CaO aluminosilicate glasses. The present samples are peralkaline
468 and peraluminous mixed Na₂O-CaO aluminosilicate glasses. Therefore, we can conclude that
469 the decrease in signal intensity is related to higher disorder in the Cl environment and is a
470 mixed cation effect that depends additionally on the aluminum content or on a deficit in
471 network-modifying Na and Ca cations.

472 The size of the electric field gradient and the large distribution of chemical shift for ³⁵Cl
473 combined with the low solubility of Cl in aluminosilicate melts (Caroll 2005) mean that the
474 information that can be obtained about the ³⁵Cl environment with MAS NMR is limited, even
475 at the highest available magnetic fields. Despite these analytical difficulties we were able to
476 show that the incorporation mechanisms of Cl in peralkaline and peraluminous
477 Na₂O-CaO-Al₂O₃-SiO₂ glasses are similar but not identical.

478

479

IMPLICATIONS

480 The NMR measurements in this study were conducted on silicate glasses and, thus, might be
481 not fully applicable to silicate melts at elevated temperatures. However, some consideration
482 about melt structure and melt viscosity can be made with caution, when the viscosity was
483 measured above and below the glass transition range on samples with a similar composition.
484 Baasner et al. (2013a) found an increase in viscosity due to the addition of Cl in peralkaline
485 Na₂O-CaO aluminosilicate melts with similar compositions to the present samples, which is
486 consistent with an increase in polymerization of the glass network indicated by the decrease in
487 chemical shift of the ²⁹Si peak when Cl is present. However, they also found that Cl decreases
488 viscosity in peraluminous Na₂O-CaO aluminosilicate melts. Theoretically, the formation of
489 Na-Ca-Cl sites as discussed in this study could decrease viscosity in peraluminous melts due
490 to reduction of charge-balancing cations and the resulting transformation of ^{IV}Al to ^VAl. ^{VI}Al
491 could decrease viscosity because the Al-O bond length is longer than in tetrahedral

20

492 coordinated ^{IV}Al (Tossel 1993) and, therefore, weaker. Indeed, several studies showed that in
493 aluminosilicate melts, after the viscosity reached its maximum at the subaluminous join, it
494 decreases with increasing peraluminosity (Riebling 1966; Toplis et al. 1997; Webb et al.
495 2007). We calculated how the removal of network-modifying cations in peralkaline melts as
496 well as the removal of charge-balancing cations in peraluminous melts due the formation of
497 Na-Ca-Cl environments would influence the R value ($\text{Na}_2\text{O}+\text{CaO}/[\text{Na}_2\text{O}+\text{CaO}+\text{Al}_2\text{O}_3]$) and
498 then calculated the theoretical change in viscosity for melts in the system
499 $\text{Na}_2\text{O}-\text{CaO}-\text{Al}_2\text{O}_3-\text{SiO}_2$ from Webb et al. (2007). From this simple approach the expected
500 change in viscosity compared to the halogen-free melts is ~ -0.02 log units for the
501 peraluminous sample ANCS 0.6Cl and $\sim +0.20$ log units for the peralkaline sample NACS
502 1.1Cl (1 log unit = a factor of 10 in viscosity in Pa s). In contrast the viscosity measurements
503 of these samples by Baasner et al. (2013a) showed that compared to the halogen-free melts Cl
504 decreases viscosity by 0.34 log units for ANCS 0.6Cl and increases viscosity by 0.96 log units
505 for NACS 1.1Cl. In both cases the comparison of such estimates with real viscosity data of
506 the present samples from Baasner et al. (2013a) showed that the measured effect of Cl on
507 viscosity is larger than expected from simple structural considerations.

508 Baasner et al. (2014) investigated the incorporation of F in peralkaline and peraluminous
509 glasses with the same composition as in the present study with MAS NMR spectroscopy.
510 Their major findings were that F in peralkaline glasses exists in environments with Na and Ca
511 as well as Al and Si, while in peraluminous glasses F only bonds to Al and Si. Our study here
512 and also those of Stebbins and Du (2002) and Sandland et al. (2004) found no strong evidence
513 for an important role of Al or Si in the incorporation mechanism of Cl in aluminosilicate
514 glasses. Therefore, one can conclude that although F and Cl are both halogens their
515 incorporation mechanisms are significantly different.

516

ACKNOWLEDGEMENTS

517 We thank the NMR team at Warwick University for their assistance in collecting the NMR
518 spectra. ³⁵Cl MAS NMR spectra at 19.6 T were acquired at the National High Magnetic Field
519 Laboratory, which is supported by the National Science Foundation (DMR-0084173) and the
520 State of Florida. We also thank Klaus Simon at University of Göttingen, who kindly
521 performed the LA-ICPMS measurements. Finally, we want to thank the editor and the two
522 reviewers for their constructive review. This project was funded by the German Research
523 Foundation, DFG grant WE 1810/9-1.

524

525

REFERENCES CITED

526 Aiuppa, A., Baker, D.R., and Webster, J.D. (2009) Halogens in volcanic systems. *Chemical*
527 *Geology* 263, 1-18.

528 Allwardt, J.R., Lee, S.K., and Stebbins, J.F. (2003) Bonding preferences of non-bridging O
529 atoms: Evidence from ¹⁷O MAS and 3QMAS NMR on calcium aluminate and
530 low-silica Ca-aluminosilicate glasses. *American Mineralogist* 88, 949-954.

531 Anderko, A., and Pitzer, K.S. (1993) Equation-of-state representation of phase equilibria and
532 volumetric properties of the system NaCl-H₂O above 573 K. *Geochimica*
533 *Cosmochimica Acta* 57, 1657-1680.

534 Baasner, A., Schmidt, B.C., and Webb, S.L. (2013a) Compositional dependence of the
535 rheology of halogen (F, Cl) bearing aluminosilicate melts. *Chemical Geology* 346,
536 172-183.

537 Baasner, A., Schmidt, B.C., and Webb, S.L. (2013b) The effect of chlorine, fluorine and
538 water on the viscosity of aluminosilicate melts. *Chemical Geology* 357, 134-149.

- 539 Baasner, A., Schmidt, B.C., Dupree, R., and Webb, S.L. (2014) Fluorine speciation as a
540 function of composition in peralkaline and peraluminous $\text{Na}_2\text{O-CaO-Al}_2\text{O}_3\text{-SiO}_2$
541 glasses: A multinuclear NMR study. *Geochimica Cosmochimica Acta*
542 <http://dx.doi.org/10.1016/j.gca.2014.01.041>.
- 543 Candela, P.A. (1997) A review of shallow, ore-related granites: Textures, volatiles, and ore
544 metals. *Journal of Petrology* 38, 1619-1633.
- 545 Carroll, M.R. (2005) Chlorine solubility in evolved alkaline magmas. *Annals of Geophysics*
546 48, 619-631.
- 547 Dingwell, D.B., and Hess, K.-U. (1998) Melt viscosities in the system Na-Fe-Si-O-Cl:
548 Contrasting effects of F and Cl in alkaline melts. *American Mineralogist* 83,
549 1016-1021.
- 550 Engelhardt, G., and Michel, D. (1987) High-resolution solid-state NMR of silicates and
551 zeolites, 485 p. John Wiley & Sons, Chichester.
- 552 Evans, K.A., Mavrogenes, J.A., O'Neill, H.S., Keller, N.S., and Jang, L.-Y. (2008) A
553 preliminary investigation of Cl XANES in silicate glasses. *Geochemistry Geophysics*
554 *Geosystems* 9, No. 10, 1-15.
- 555 Freude, D., and Haase, J. (1993) Quadrupole effects in solid state nuclear magnetic resonance.
556 In P. Diehl, E. Flunck, H. Günther, R. Kosfeld, J. Seelig, Eds., *NMR basic principles*
557 *and progress*, Vol. 29, p. 1-90. Springer, New York.
- 558 Gervais, C., Dupree, R., Pike, K.J., Bonhomme, C., Profeta, M., Pickard, C.J., Mauri, F.
559 (2005) Combined First-Principles Computational and Experimental Multinuclear
560 Solid-State NMR Investigation of Amino Acids. *The Journal of Physical Chemistry A*
561 109 (31), 6960-6969.

- 562 Helgeson, H.C. (1969) Thermodynamics of hydrothermal systems at elevated temperatures
563 and pressures. *American Journal of Science* 267, 729-804.
- 564 Johnson, K.J., Hunt, J.P., and Dodgen, H.W. (1969) Chlorine-35 NMR study of the shifts and
565 line shapes of some liquid inorganic chlorides. *Journal of Chemical Physics* 51,
566 4493-4496.
- 567 Karpukhina, N., Law, R.V., Hill, R.G. (2008) Solid state NMR study of calcium fluorosilicate
568 glasses. *Advanced Materials Research* 39-40, 25-30.
- 569 Kemp, T.F., and Smith, M.E. (2009) QuadFit - A new cross-platform computer program for
570 simulation of NMR line shapes from solids with distributions of interaction parameters.
571 *Solid State Nuclear Magnetic Resonance* 35, 243-252.
- 572 Kiczenski, T.J., Stebbins, J.F.(2002) Fluorine sites in calcium and barium oxyfluorides: F-19
573 NMR on crystalline model compounds and glasses. *Journal of Non-Crystalline Solids*
574 306, 160-168.
- 575 Kirkpatrick, R.J. (1988) MAS NMR spectroscopy of minerals and glasses. In F.C.
576 Hawthorne, Ed., *Spectroscopic methods in mineralogy and geology*, *Reviews in*
577 *Mineralogy* 18, p. 341-429. Mineralogical Society of America, Washington D.C..
- 578 Kohn, S.C., Dupree, R., Mortuza, M.G., and Henderson, C.M.B. (1991) NMR evidence for
579 five- and six-coordinated aluminum fluoride complexes in F-bearing aluminosilicate
580 glasses. *American Mineralogist* 76, 309-312.
- 581 Lee, S.K. (2004) Structure of silicate glasses and melts at high pressure: Quantum chemical
582 calculations and solid-state NMR. *The Journal of Physical Chemistry B* 108,
583 5889-5900.

- 584 Lee, S.K., and Stebbins, J.F. (2009) Effects of the degree of polymerization on the structure of
585 sodium silicate and aluminosilicate glasses and melts: An ^{17}O NMR study.
586 *Geochimica Cosmochimica Acta* 73, 1109-1119.
- 587 Lucken, E.A. (1969) Nuclear Quadrupole Coupling Constants. Academic Press, London.
- 588 Marsmann, H.C., Meyer, E., Vongehr, M., and Weber, E.F. (1983) ^{29}Si
589 NMR-Untersuchungen an Polykieselsäureestern. *Die Makromolekulare Chemie* 184,
590 1817-1822.
- 591 Massiot, D., Bessada, C., Coutures, J.P., and Taulelle, F. (1990) A quantitative study of ^{27}Al
592 MAS NMR in crystalline YAG. *Journal of Magnetic Resonance* 90, 231-242.
- 593 Mysen, B.O., Cody, G.D., Smith, A.(2004) Solubility mechanism of fluorine in peralkaline
594 and meta-aluminous silicate glasses and in melts to magmatic temperatures.
595 *Geochimica Cosmochimica Acta* 68, 2745-2769.
- 596 Riebling, E.F.(1966) Structure of sodium aluminosilicate melts containing at least 50 mole%
597 SiO_2 at 1500°C. *Journal of Chemical Physics* 44, 2857-2865.
- 598
- 599 Sandland, T.O., Du, L.-S., Stebbins, J.F., and Webster, J.D. (2004) Structure of
600 Cl-containing silicate and aluminosilicate glasses: A ^{35}Cl MAS-NMR study.
601 *Geochimica Cosmochimica Acta* 68, 5059-5069.
- 602 Signorelli, S., and Carroll, M.R. (2000) Solubility and fluid-melt partitioning of Cl in hydrous
603 phonolitic melts. *Geochimica Cosmochimica Acta* 64, 2851-2862.
- 604 Schaller, T., Dingwell, D.B., Keppler, H., Knöller W., Merwin, L., and Sebal, A.(1992)
605 Fluorine in silicate glasses: A multinuclear magnetic resonance study. *Geochimica*
606 *Cosmochimica Acta* 56, 701-707.

- 607 Schmidt, B.C., Riemer, T., Kohn, S.C., Behrens, H., and Dupree, R. (2000a) Different water
608 solubility mechanisms in hydrous glasses along the Qz-Ab join: Evidence from NMR
609 spectroscopy. *Geochimica Cosmochimica Acta* 64, 513-526.
- 610 Schmidt, B.C., Riemer, T., Kohn, S.C., Behrens H., and Dupree, R. (2000b) Erratum to
611 “Different water solubility mechanisms in hydrous glasses along the Qz-Ab join:
612 Evidence from NMR spectroscopy”. *Geochimica Cosmochimica Acta* 64, 2895-2896.
- 613 Schmäcker, M., MacKenzie, K.J.D., Schneider, H., and Meinhold, R. (1997) NMR studies on
614 rapidly solidified SiO₂-Al₂O₃ and SiO₂-Al₂O₃-Na₂O-glasses. *Journal of*
615 *Non-Crystalline Solids* 217, 99-105.
- 616 Sourirajan, S., and Kennedy, G.C. (1962) The system H₂O-NaCl at elevated temperatures and
617 pressures. *American Journal of Science* 260, 115-141.
- 618 Stamboulis, A., Hill, R.G., Law, R.V. (2005) Structural characterization of fluorine
619 containing glasses by ¹⁹F, ²⁷Al, ²⁹Si and ³¹P MAS-NMR spectroscopy. *Journal of Non-*
620 *Crystalline Solids* 351, 3289-3295.
- 621 Stebbins, J.F. (1995) Dynamics and structure of silicate and oxide melts: nuclear magnetic
622 resonance studies. In J.F. Stebbins, P.F. McMillan, D.B. Dingwell, Eds., *Structure,*
623 *dynamics and properties of silicate melts, Reviews in Mineralogy* 32, p. 191-246.
624 Mineralogical Society of America, Washington D.C..
- 625 Stebbins, J.F., Xu, Z., 1997. NMR evidence for excess non-bridging oxygen in an
626 aluminosilicate glass. *Nature* 390, 60-61.
- 627 Stebbins, J.F., Zeng, Q. (2000) Cation ordering at fluoride sites in silicate glasses: a high-
628 resolution ¹⁹F NMR study. *Journal of Non-Crystalline Solids* 262, 1-5.

- 629 Stebbins, J.F., Kroeker, S., Lee, S.K., Kiczenski, T.J. (2000) Quantification of five- and six-
630 coordinated aluminium ions in aluminosilicate and fluoride-containing glasses by
631 high- field, high-resolution ^{27}Al NMR. *Journal of Non-Crystalline Solids* 275, 1-6.
- 632 Stebbins, J.F., and Du, L.-S. (2002) Chloride ion sites in silicate and aluminosilicate glasses:
633 A preliminary study by ^{35}Cl solid-state NMR. *American Mineralogist* 87, 359-363.
- 634 Tanimoto, S., and Rehren, T. (2008) Interactions between silicate and salt melts in LBA
635 glassmaking. *Journal of Archaeology Sci.* 35, 2566-2573.
- 636 Thompson, L., and Stebbins, J.F. (2011) Non-bridging oxygen and high-coordinated
637 aluminum in metaluminous and peraluminous calcium and potassium aluminosilicate
638 glasses: High-resolution ^{17}O and ^{27}Al MAS NMR results. *American Mineralogist* 96,
639 841-853.
- 640 Toplis, M.J., Dingwell, D.B., and Lenci, T. (1997) Peraluminous viscosity maxima in
641 $\text{Na}_2\text{O}-\text{Al}_2\text{O}_3-\text{SiO}_2$ liquids: The role of triclusters in tectosilicate melts. *Geochimica*
642 *Cosmochimica Acta* 61, 2605-2612.
- 643 Tossel, J.A. (1993) Theoretical studies of the speciation of Al in F-bearing aluminosilicate
644 glasses. *American Mineralogist* 78, 16-22.
- 645 Webb, S.L., Banaszak, M., Köhler, U., Rausch S., and Raschke, G. (2007) The viscosity of
646 $\text{Na}_2\text{O}-\text{CaO}-\text{Al}_2\text{O}_3-\text{SiO}_2$ melts. *European Journal of Mineralogy* 19, 681-692.
- 647 Webster, J.D. (1997a) Exsolution of magmatic volatile phases from Cl-enriched mineralizing
648 granitic magmas and implications for ore metal transport. *Geochimica Cosmochimica*
649 *Acta* 61, 1017-1029.
- 650 Webster, J.D. (1997b) Chloride solubility in felsic melts and the role of chloride in magmatic
651 degassing. *Journal of Petrology* 38, 1793-1807.

652 Zeng, Q., Stebbins, J.F. (2000) Fluoride sites in aluminosilicate glasses: High-resolution ^{19}F
653 NMR results. American Mineralogist 85, 863-867.

654 Zimova, M., and Webb, S.L., 2006. The effect of chlorine on the viscosity of
655 $\text{Na}_2\text{O}-\text{Fe}_2\text{O}_3-\text{Al}_2\text{O}_3-\text{SiO}_2$ melts. American Mineralogist 91, 344-352.

656

657 **FIGURE CAPTIONS**

658

659 Figure 1. ^{35}Cl MAS NMR spectra of the Cl- and F-bearing peraluminous, peralkaline and
660 sodium silicate glasses at 14.1 T. Spinning sidebands are marked with an asterisk. The spectra
661 are normalized to the same peak height.

662

663 Figure 2. ^{35}Cl MAS NMR spectra of the Cl- and F-bearing peraluminous, peralkaline and
664 sodium silicate glasses at 19.6 T. Spinning sidebands are marked with an asterisk. The spectra
665 are normalized to the same peak height. The small peak at 75 ppm in the spectrum of NACS
666 1.1Cl is a contamination with an unknown material, which was not observed in the spectrum
667 of NACS 1.1Cl at 14.1 T.

668

669 Figure 3. ^{35}Cl MAS NMR spectra of the Cl-bearing peraluminous (ANCS) and peralkaline
670 (NACS) glasses at 14.1 T. Spinning sidebands are marked with an asterisk. The spectra are
671 normalized to the same number of acquisitions and same number of Cl atoms.

672

673 Figure 4. Static ^{35}Cl NMR spectra of the sodium silicate glass NS 2.2Cl and the peralkaline
674 glass NACS 1.1Cl at 14.1 T. The spectra are normalized to the same number of acquisitions
675 and same number of Cl atoms (peak maxima for both samples ~ 90 ppm).

676

677 Figure 5. ^{35}Cl MAS NMR spectra of the Cl- bearing peraluminous (ANCS) and peralkaline
678 glasses (NACS) at 14.1 T and 19.6T. Spinning sidebands are marked with an asterisk. The
679 spectra are normalized to the same peak height. The baseline is the same for all spectra. The
680 spectrum of ANCS 1.2Cl only appears to have a higher baseline because of spinning
681 sidebands.

682
683 Figure 6. Center of gravity of ^{35}Cl MAS NMR central bands of the Cl-bearing peraluminous
684 (ANCS 1.2 Cl (14.1 T)+ANCS 0.6Cl (19.6 T)), peralkaline (NACS 1.9Cl (14.1 T)+NACS
685 1.1Cl (14.1 T, 19.6 T) and sodium silicate glass as a function of inverse squared Larmor
686 frequency ν^{-2} . The ordinate of the linear regressions gives the isotropic chemical shift δ_{iso} and
687 the quadrupole coupling C_q constant is calculated from the slope. (see Table 3). The numbers
688 over the data are the magnetic fields in Tesla.

689
690 Figure 7. ^{35}Cl MAS NMR spectra of the peralkaline glass NACS 1.1Cl at 14.1 T and 19.6 T
691 (black lines) fitted with the program Quadfit (grey lines). Spinning sidebands are marked with
692 an asterisk. The spectra are normalized to the same peak height.

693
694 Figure 8. ^{23}Na MAS NMR spectra of halogen-free and halogen-bearing peraluminous and
695 peralkaline glasses at 11.7 T. The spectra are normalized to the same peak area. The small
696 peak in the high frequency flank of the peak of NACS 1.9Cl is a contamination with the
697 reference material NaCl.

698
699 Figure 9. ^{27}Al MAS NMR spectra of the Cl-free and Cl-bearing peralkaline (NACS) glasses at
700 11.7 T. The spectra are normalized to the same peak height. The residual results from
701 subtracting the spectrum of NACS from that of NACS 1.9Cl.

702

703 Figure 10. ^{27}Al MAS NMR spectra of the Cl-free and Cl-bearing peraluminous (ANCS)
704 glasses at 11.7 T. The spectra are normalized to the same peak height. The residual results
705 from subtracting the spectrum of ANCS from that of ANCS 1.2Cl.

706

707 Figure 11. ^{29}Si MAS NMR spectra of the halogen-free and halogen-bearing peraluminous and
708 peralkaline glasses at 7 T. The spectra are normalized to the same peak height.

709

710

711

712

713

714

715

716

717

718

719

720

721

722

723

724

725 Table 1a. Electron microprobe (EMP) analysis as oxide components of the glass samples. ^a

	SiO ₂	2 σ	Al ₂ O ₃	2 σ	CaO	2 σ	Na ₂ O	2 σ	F	2 σ	Cl	2 σ	R ^c	Ca/[Ca+Na]
	[mol%]	[mol%]	[mol%]	[mol%]	[mol%]	[mol%]	[mol%]	[mol%]	[mol%]	[mol%]	[mol%]	[mol%]		
Peralkaline														
NACS ^b	65.52	1.42	11.94	1.02	5.53	0.36	17.02	0.57	-	-	-	-	0.65	0.14
NACS 1.0F 1.0Cl ^b	65.77	0.27	11.95	0.10	5.50	0.10	15.79	0.17	0.99	0.15	1.02	0.04	0.64	0.15
NACS 1.1Cl ^b	66.86	0.42	11.82	0.13	5.75	0.16	15.57	0.37	-	-	1.10	0.06	0.64	0.16
NACS 1.9Cl ^b	65.55	0.31	11.95	0.16	5.81	0.10	16.69	0.17	-	-	1.92	0.06	0.65	0.15
Peraluminous														
ANCS ^d	65.94	1.63	19.20	1.07	4.19	0.39	10.67	0.25	-	-	-	-	0.44	0.16
ANCS 1.0F 0.9Cl ^b	66.48	0.80	19.73	0.55	3.84	0.12	8.95	0.25	1.01	0.19	0.88	0.02	0.39	0.18
ANCS 0.6Cl ^d	66.31	0.55	20.45	0.31	3.75	0.11	9.49	0.51	-	-	0.64	0.05	0.39	0.16
ANCS 1.2Cl ^b	67.01	0.35	18.55	0.13	4.03	0.13	10.41	0.21	-	-	1.18	0.13	0.44	0.16
Sodium silicate														
NS 2.2Cl ^b	78.09	1.10	0.44	0.05	0.04	0.03	21.43	0.67	-	-	2.20	0.50	-	-

726 a - Standards were: Wollastonite = Si, Ca; Anorthite = Al; Albite = Na, Topaz = F; Halite = Cl.; Sanidine = K, Cobalt oxide = Co. In all samples
727 contaminations of K₂O (< 0.1 mol%) from the SiO₂ and Al₂O₃ chemicals were observed.

728 b - Doped with < 0.12 mol% CoO.

729 c - R = (Na₂O+CaO)/(Na₂O+CaO+Al₂O₃) in mole fraction is an measure of the degree of polymerization of the melt by taking into account the
730 number of sodium and calcium that is either used for charge-balancing aluminum or creating non-bridging oxygens in the melt (e.g. Thompson and
731 Stebbins, 2011). If R > 0.5 the glass is peralkaline and if R < 0.5 the glass is peraluminous.

732 d - Published in Baasner et al. (2013a)

733

734

735

736

737

738 Table 1b. Electron microprobe (EMP) analysis of the glass samples.^a

	Si	2 σ	Al	2 σ	Ca	2 σ	Na	2 σ	F	2 σ	Cl	2 σ	O ^c	Ca/[Ca+Na]
	[at%]	[at%]	[at%]	[at%]	[at%]	[at%]	[at%]	[at%]	[at%]	[at%]	[at%]	[at%]	[at%]	
Peralkaline														
NACS ^b	20.58	0.45	7.50	0.64	1.74	0.11	10.69	0.36	-	-	-	-	59.49	0.14
NACS 1.0F 1.0Cl ^b	20.79	0.09	7.55	0.06	1.74	0.03	9.98	0.10	0.31	0.05	0.32	0.012	59.31	0.15
NACS 1.1Cl ^b	21.00	0.13	7.42	0.08	1.81	0.05	9.78	0.23	-	-	0.34	0.019	59.65	0.16
NACS 1.9Cl ^b	20.54	0.10	7.49	0.10	1.82	0.03	10.46	0.11	-	-	0.60	0.018	59.08	0.15
Peraluminous														
ANCS ^d	19.73	0.49	11.49	0.64	1.25	0.12	6.38	0.15	-	-	-	-	61.14	0.16
ANCS 1.0F 0.9Cl ^b	19.93	0.24	11.83	0.33	1.15	0.04	5.37	0.15	0.30	0.06	0.26	0.006	61.16	0.18
ANCS 0.6Cl ^d	19.65	0.16	12.12	0.18	1.11	0.03	5.62	0.30	-	-	0.19	0.014	61.31	0.16
ANCS 1.2Cl ^b	20.08	0.10	11.12	0.08	1.21	0.04	6.24	0.13	-	-	0.36	0.040	60.99	0.16
Sodium silicate														
NS 2.2Cl ^b	25.86	0.37	0.29	0.04	0.01	0.01	14.20	0.44	-	-	0.73	0.165	58.91	-

739 a - Standards were: Wollastonite = Si, Ca; Anorthite = Al; Albite = Na, Topaz = F; Halite = Cl.; Sanidine = K, Cobaltoxide = Co. In all samples
740 contaminations of K (< 0.03 at%) from the SiO₂ and Al₂O₃ chemicals were observed.

741 b - Doped with < 0.04 at% Co.

742 c - Calculated from stoichiometry by taking in account that two F⁻¹ replace one O⁻² in the glass.

743 d - Published in Baasner et al. (2013a)

744

745

746

747

748 | Table 2. ^{35}Cl peak maximum, center of gravity and full width half maximum $FWHM$ of the
 749 ^{35}Cl MAS NMR spectra at different fields ^a.

Formatted: Numbering: Continuous

	Peak maximum [ppm]		Center of gravity [ppm]		$FWHM$ [ppm]	
	14.1 T	19.6 T	14.1 T	19.6 T	14.1 T	19.6 T
Peralkaline						
NACS 1.0F 1.0Cl	-132	-112	-149	-128	151	109
NACS 1.1Cl	-131	-117	-155	-129	145	104
NACS 1.1Cl ^b	-130	-	-161	-	161	-
NACS 1.9Cl	-123	-	-163	-	165	-
Peraluminous						
ANCS 1.0F 0.9Cl	-119	-104	-143	-115	191	182
ANCS 0.6Cl	-152	-130	-123	-113	303	139
ANCS 1.2Cl	-123	-	-149	-	246	-
Sodium silicate						
NS 2.2Cl	-137	-109	-156	-129	103	74

750 a - The errors of the peak maximum and center of gravity are ± 5 ppm for the 14.1 T spectra
 751 and ± 3 ppm for the 19.6 T spectra. The error in $FWHM$ is less than ± 16 ppm for the
 752 peralkaline samples, but ± 25 ppm for the peraluminous samples because of the low signal to
 753 noise ratio.

754 b - measured on the Varian spectrometer 14.1 T

755
 756

757 Table 3. ^{35}Cl isotropic chemical shift δ_{iso} , width due to quadrupole broadening W_q , width due
 758 to chemical shift distribution W_{csd} and quadrupole coupling constant C_q obtained from spectra
 759 ^{35}Cl MAS spectra at 14.1 T and 19.6 T evaluated after Schmidt et al. (2000a, b).

	δ_{iso} ^a	C_q ^b	W_q ^c	W_{csd} ^c
	[ppm]	[MHz]	[ppm] 14.1 T	[ppm] 14.1 T
Peralkaline				
NACS 1.0F 1.0Cl	-105	2.3	123	89
NACS 1.1Cl + NACS 1.9Cl ^d	-95	2.8	131	79
Peraluminous				
ANCS 1.0F 0.9Cl ^f	-74	3.1	-	-
ANCS 0.6Cl + ANCS 1.2Cl ^{ef}	-75	3.0	-	-
Sodium silicate				
NS 2.2Cl	-101	2.6	84	60

760 a - The maximum error in δ_{iso} is ± 16 ppm.

761 b - C_q was calculated estimating an asymmetry parameter $\eta = 0.7$. The maximum error in C_q
 762 is ± 0.3 MHz taking into account that η could range from 0 to 1.

763 c - The maximum error in W_q and W_{CSD} is less than $\pm 12.5\%$ for a max. error of 16 ppm in
 764 $FWHM$.

765 d - The evaluation was done based on the measurements of the sample NACS 1.1Cl at 14.1 T
 766 and 19.6 T and the sample NACS 1.9Cl at 14.1 T.

767 e - The spectrum of ANCS 0.6Cl at 14.1 T was not included in the evaluation for δ_{iso} and C_q
 768 because of its poor/low signal to noise ratio. The evaluation was done based on the
 769 measurement of ANCS 1.2Cl at 14.1 T and ANCS 0.6Cl at 19.6T.

770 f - W_q and W_{CSD} are not presented for the peraluminous spectra because of their low signal to
 771 noise ratio.

772
 773
 774

775 Table 4. ^{35}Cl chemical shift δ_{iso} , width due to chemical shift distribution W_{csd} and quadrupole
 776 coupling constant \bar{C}_q , the quadrupole distribution $\Delta\bar{C}_q$, the asymmetry parameter η and the
 777 distribution of the asymmetry parameter $\Delta\eta$ of the curves fitted to the ^{35}Cl MAS NMR spectra
 778 at different magnetic fields B with the program Quadfit^a.

	δ_{iso}	W_{csd}	\bar{C}_q	$\Delta\bar{C}_q$	$\bar{\eta}$	$\Delta\bar{\eta}$
	[ppm]	[ppm]	[MHz]	[MHz]		
ANCS 1.0F 0.9Cl	-45	125	4.2	3.0	0.8	0.2
ANCS 0.6Cl	-58	125	4.3	3.0	0.8	0.2
ANCS 1.2Cl	-30	125	4.2	3.0	0.8	0.2
NACS 1.0F 1.0Cl	-79	72	3.3	2.1	0.8	0.2
NACS 1.1Cl	-77	82	3.7	2.7	0.5	0.2
NACS 1.9Cl	-74	82	3.5	3.0	0.7	0.2
NS 2.2Cl	-80	37	3.5	2.5	0.5	0.3

779 a - Various approaches to fit the spectra suggest that the errors of the parameter are ± 5 ppm
 780 for $\delta_{iso} \pm 10$ ppm for W_{csd} , 0.2 for $\bar{\eta}$, 0.1 for $\Delta\bar{\eta}$ and ± 0.2 MHz for $\Delta\bar{C}_q$ and $\Delta\bar{C}_q$.

781
 782

783 Table 5. ^{23}Na peak maximum, center of gravity and full width half maximum $FWHM$ of the
 784 ^{23}Na MAS NMR spectra at 11.7 T^a.

	Peak maximum	Center of gravity	$FWHM$
	[ppm]	[ppm]	[ppm]
NACS ^b	-17.0	-16.9	25.7
NACS 1.0Cl 1.0F	-16.0	-16.6	24.4
NACS 1.1Cl	-16.3	-16.8	24.7
NACS 1.9Cl	-14.9	-16.7	25.2
ANCS ^b	-20.7	-19.2	20.7
ANCS 0.9Cl 1.0F	-20.6	-20.8	20.9
ANCS 1.2Cl	-18.8	-19.2	20.9

785 a - The errors of peak maximum, center of gravity and $FWHM$ are ± 0.5 ppm.

786 b - from Baasner et al. (2014)

787
 788

789 Table 6. ^{27}Al peak maximum, center of gravity and full width half maximum $FWHM$ of the
 790 ^{27}Al MAS NMR spectra at different magnetic fields^a.

	Magnetic field	Peak maximum	Center of gravity	$FWHM$
	[T]	[ppm]	[ppm]	[ppm]
NACS ^b	11.7	55.54	51.18	16.90
NACS 1.1Cl	11.7	55.36	52.54	16.96
NACS 1.9Cl	11.7	55.28	51.71	16.81
ANCS ^b	11.7	52.55	43.91	23.21
ANCS1.2Cl	11.7	52.82	41.57	23.89
ANCS ^b	20.0	57.03	54.30	15.04
ANCS 1.2Cl	20.0	57.17	54.21	15.25

791 a - The errors of peak maximum, center of gravity and $FWHM$ are ± 0.25 ppm for the 11.7 and
 792 20 T spectra.

793 b - from Baasner et al. (2014)

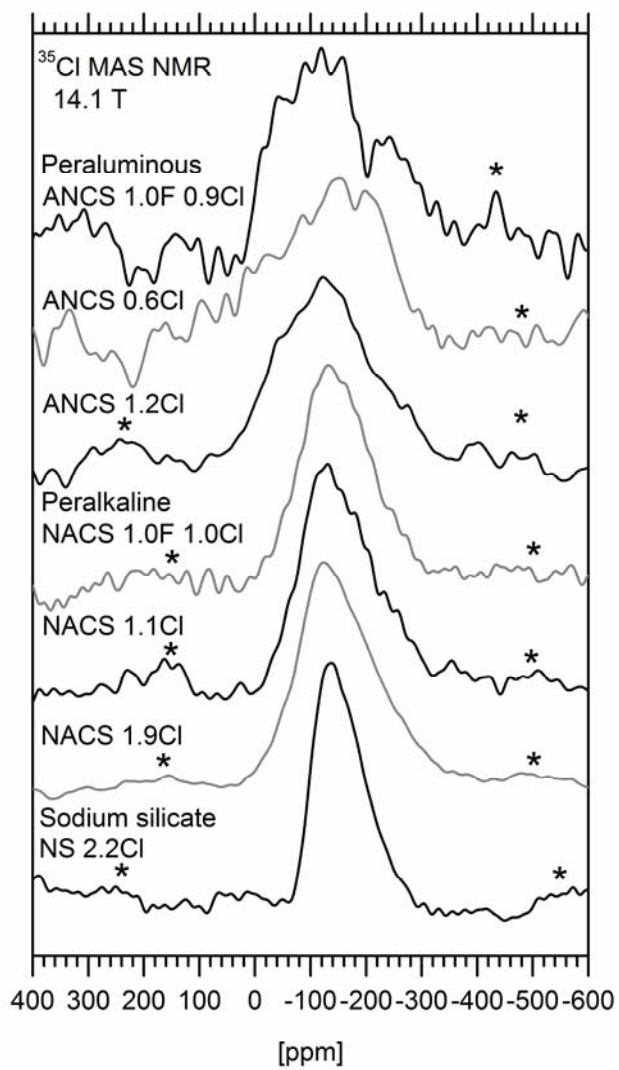
794
 795
 796
 797

798
799
800
801
802
803
804
805
806
807
808
809

Table 7. ^{29}Si isotropic chemical shift δ_{iso} , center of gravity and full width half maximum ($FWHM$) of the ^{29}Si MAS NMR spectra at 7 T^a.

	δ_{iso} [ppm]	Center of gravity [ppm]	$FWHM$ [ppm]
NACS ^b	-96.3	-96.2	17.1
NACS 1.0Cl 1.0F	-97.2	-97.9	17.1
NACS 1.1Cl	-97.2	-97.9	17.5
ANCS ^b	-100.4	-100.4	17.9
ANCS 0.9Cl 1.0F	-100.8	-101.1	18.0

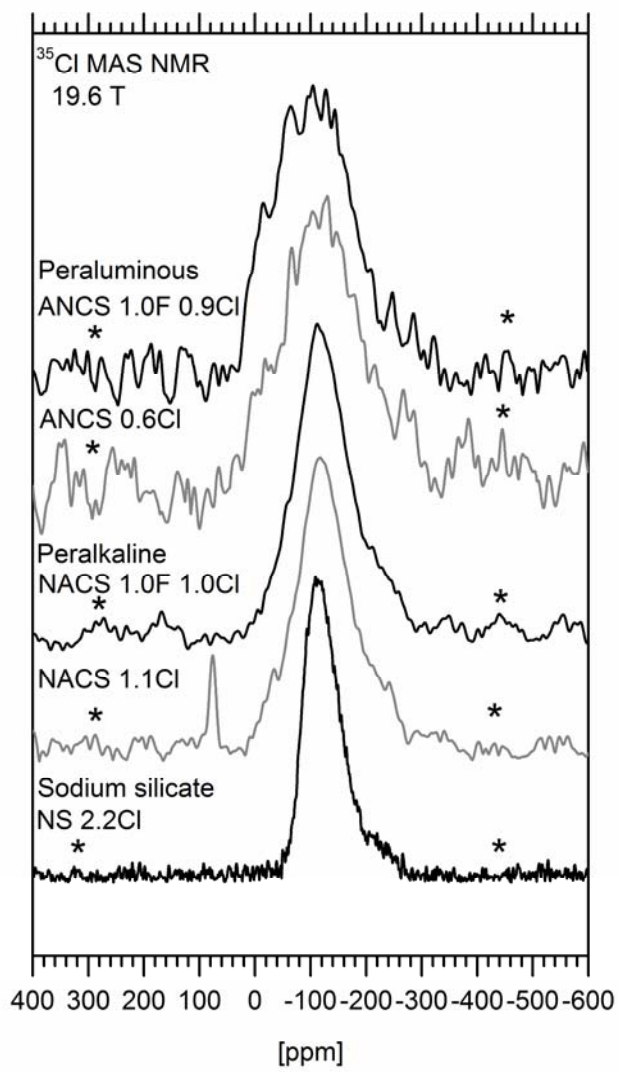
a - The errors of δ_{iso} , center of gravity and $FWHM$ are ± 0.4 ppm.
b - from Baasner et al. (2014)



810

811 Figure 1.

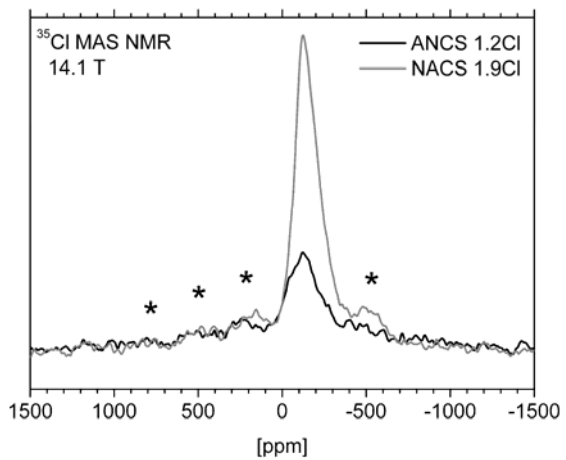
812



813

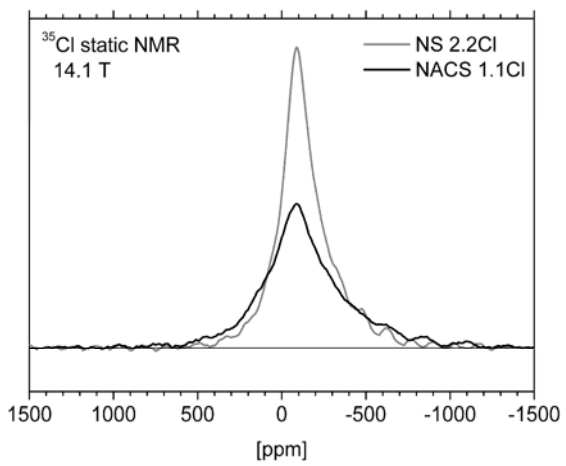
814 Figure 2.

815



816

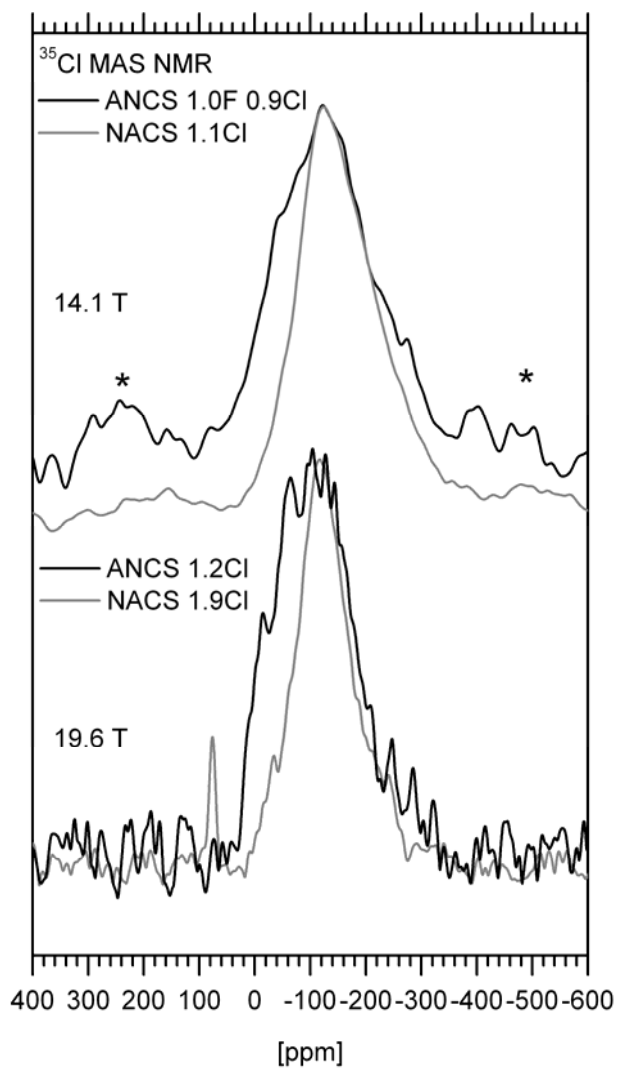
817 Figure 3.



818

819 Figure 4.

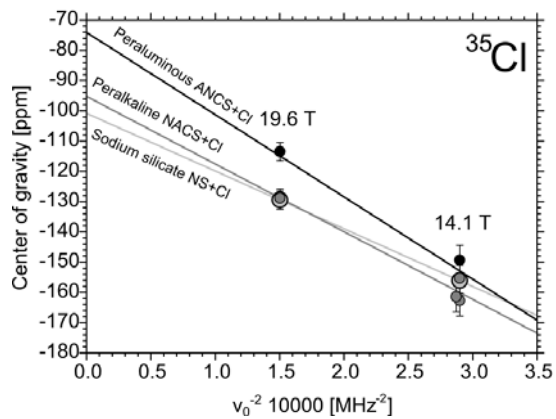
820



821

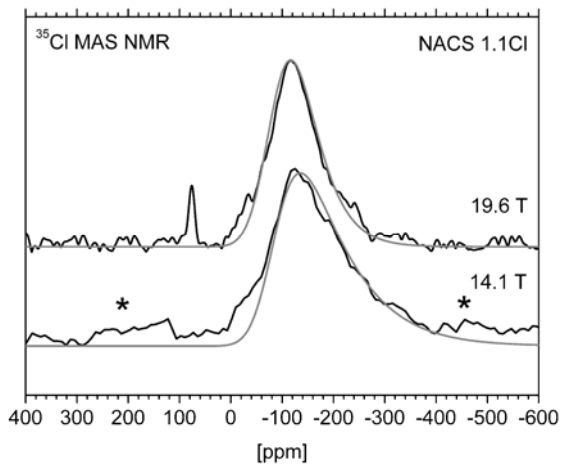
822 Figure 5.

823

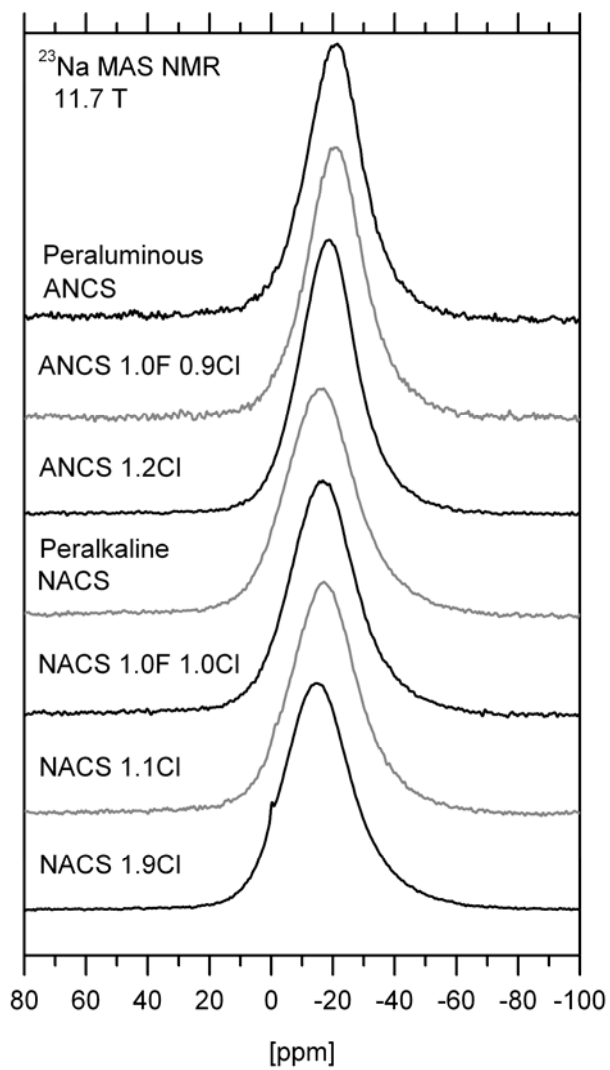


824
825 Figure 6.

826



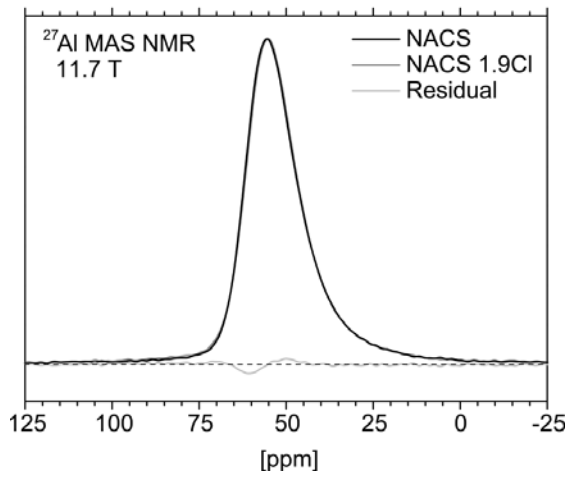
827
828 Figure 7.



829

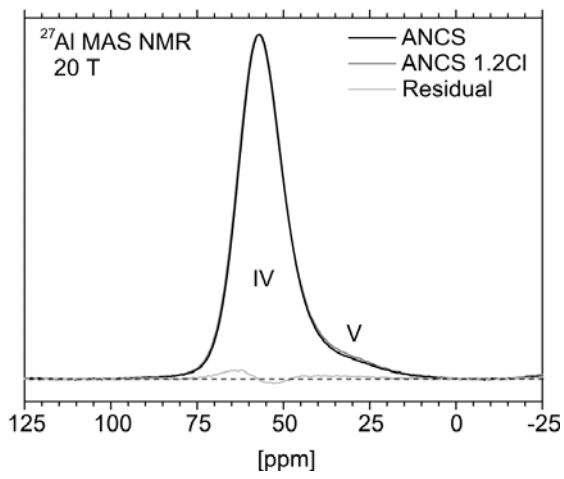
830 Figure 8.

831



832

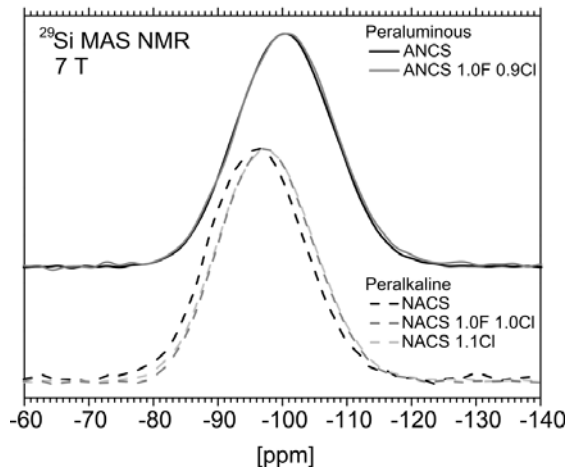
833 Figure 9.



834

835 Figure 10.

836



837

838 Figure 11.

839

840

841

842

843

844

845

846

847

848

849

850

851

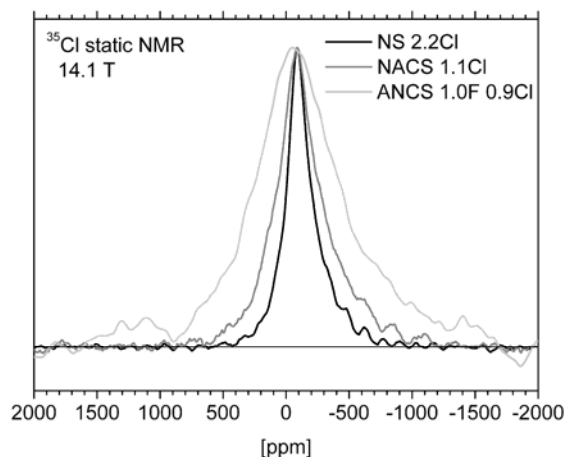
852

853

854

855 SUPPLEMENTARY DATA

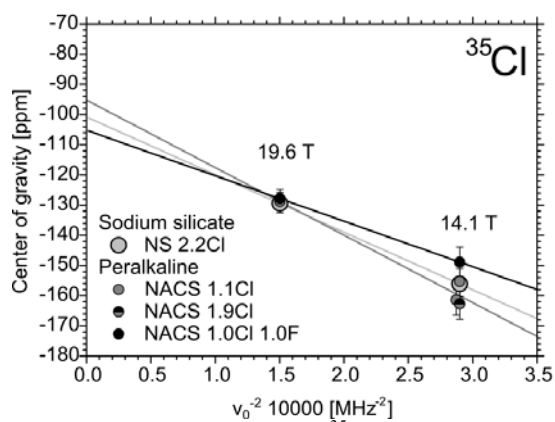
856



857

858 Figure A. Static ^{35}Cl NMR spectra of the sodium silicate glass NS 2.2Cl, the peralkaline glass
 859 NACS 1.1Cl and the peraluminous glass ANCS 1.0F 0.9Cl at 14.1 T. The peak maxima are
 860 at -90 ppm for the sodium silicate and the peralkaline glass and -50 ppm for the peraluminous
 861 glass. The spectra are normalized to the same peak height.

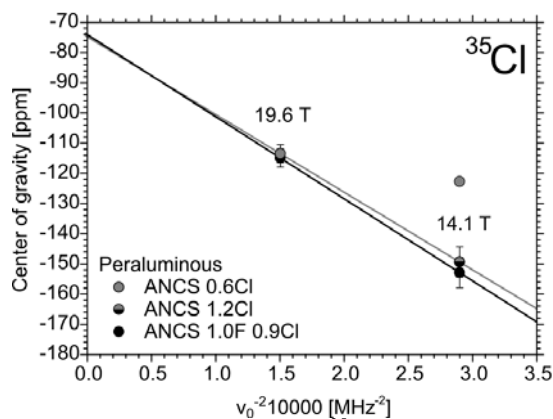
862



863

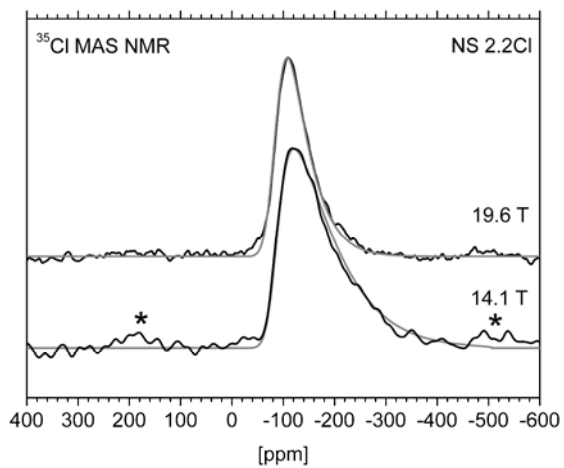
864 Figure B. Center of gravity of ^{35}Cl MAS NMR central bands of the Cl-bearing peralkaline and
 865 sodium silicate glasses as a function of inverse squared Larmor frequency ν^{-2} . The ordinate of
 866 linear regressions gives the isotropic chemical shift δ_{iso} and the quadrupole coupling C_q
 867 constant was calculated from the slope (see Table 3). The numbers on top of the data are the

868 magnetic fields in Tesla. One linear equation was fitted to the combined data of NACS 1.1Cl
869 at 14.1 T, 19.6 T and NACS 1.9Cl at 14.1 T.



870
871 Figure C. Center of gravity of ^{35}Cl MAS NMR central bands of the Cl-bearing peralkaline and
872 sodium silicate glasses as a function of inverse squared Larmor frequency ν^{-2} . The ordinate of
873 the linear regressions gives the isotropic chemical shift δ_{iso} and the quadrupole coupling C_q
874 constant was calculated from the slope (see Table 3). The numbers on top of the data are the
875 magnetic fields in Tesla. The center of gravity of ANCS 0.6Cl at 14.1 T was not used for
876 further evaluation as the signal to noise ratio of the spectrum was too low and its usage in
877 evaluation delivered an unusual low $C_q \sim 1.5$ MHz, which is not consistent with the general
878 quadrupole peak shape in the spectra in this study and previous studies (e.g. Sandland et al.,
879 2004). Instead a linear equation was fitted to the center of gravity of ANCS 1.2Cl at 14.1 T
880 and the center of gravity of ANCS 0.6Cl at 19.6 T.

881



882

883 Figure D. ^{35}Cl MAS NMR spectra of the sodium silicate glass NS 2.2Cl at 14.1 T and 19.6 T

884 (black lines) fitted with the program Quadfit (grey lines). The fit is $\overline{C}_q = 3.5$ MHz,

885 $\Delta\overline{C}_q = 2.5$ MHz, $\overline{\eta} = 0.5$, $\Delta\overline{\eta} = 0.3$. Spinning sidebands are marked with an asterisk. The

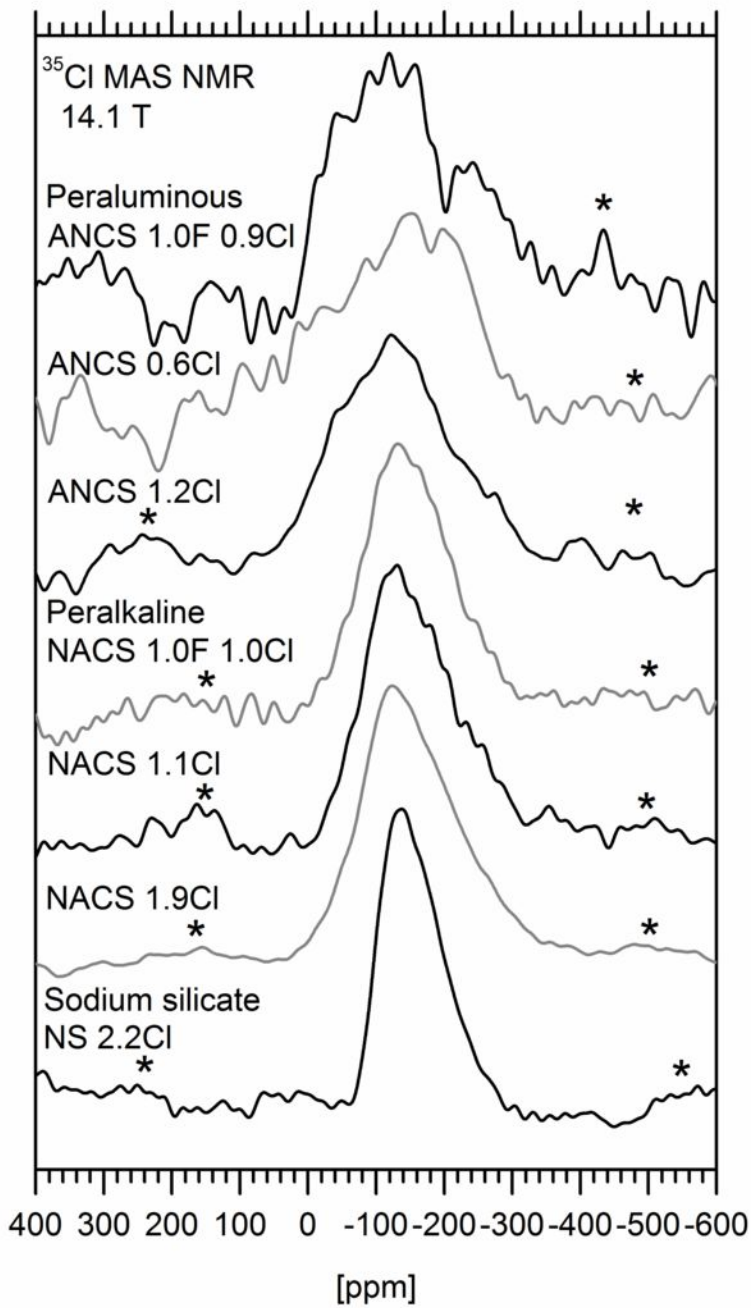
886 spectra are normalized to the same peak height.

887

888
889 Table A. Expected MAS relative intensities after Massiot et al. (1990) for a range of
890 quadrupole coupling constants C_q and an asymmetry parameter $\eta = 0.8$ for different magnetic
891 fields (values in T) and spinning speeds (values in kHz).

C_q [MHz]	Intensity	
	14.1 T 20 kHz	19.6 T 30 kHz
2.6	0.75	0.94
3.5	0.38	0.80
4.1	0.19	0.65
4.3	0.16	0.58

892
893
894
895
896



³⁵Cl MAS NMR
19.6 T

Peraluminous
ANCS 1.0F 0.9Cl
*

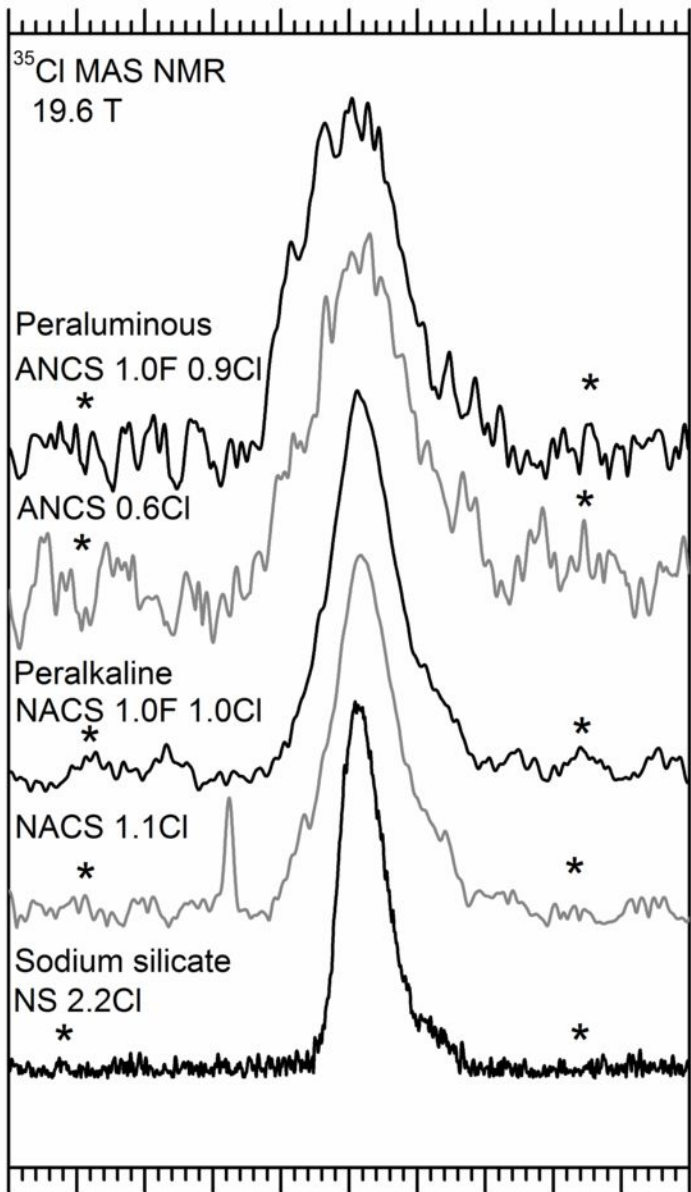
ANCS 0.6Cl
*

Peralkaline
NACS 1.0F 1.0Cl
*

NACS 1.1Cl
*

Sodium silicate
NS 2.2Cl
*

400 300 200 100 0 -100 -200 -300 -400 -500 -600
[ppm]

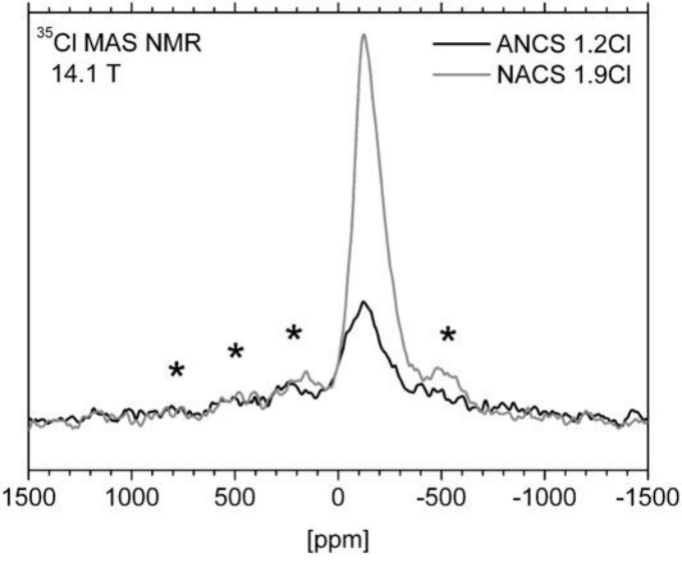


^{35}Cl MAS NMR
14.1 T

— ANCS 1.2Cl
— NACS 1.9Cl

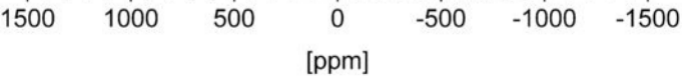
1500 1000 500 0 -500 -1000 -1500
[ppm]

* * * *



^{35}Cl static NMR
14.1 T

— NS 2.2Cl
— NACS 1.1Cl



³⁵Cl MAS NMR

— ANCS 1.0F 0.9Cl

— NACS 1.1Cl

14.1 T

*

*

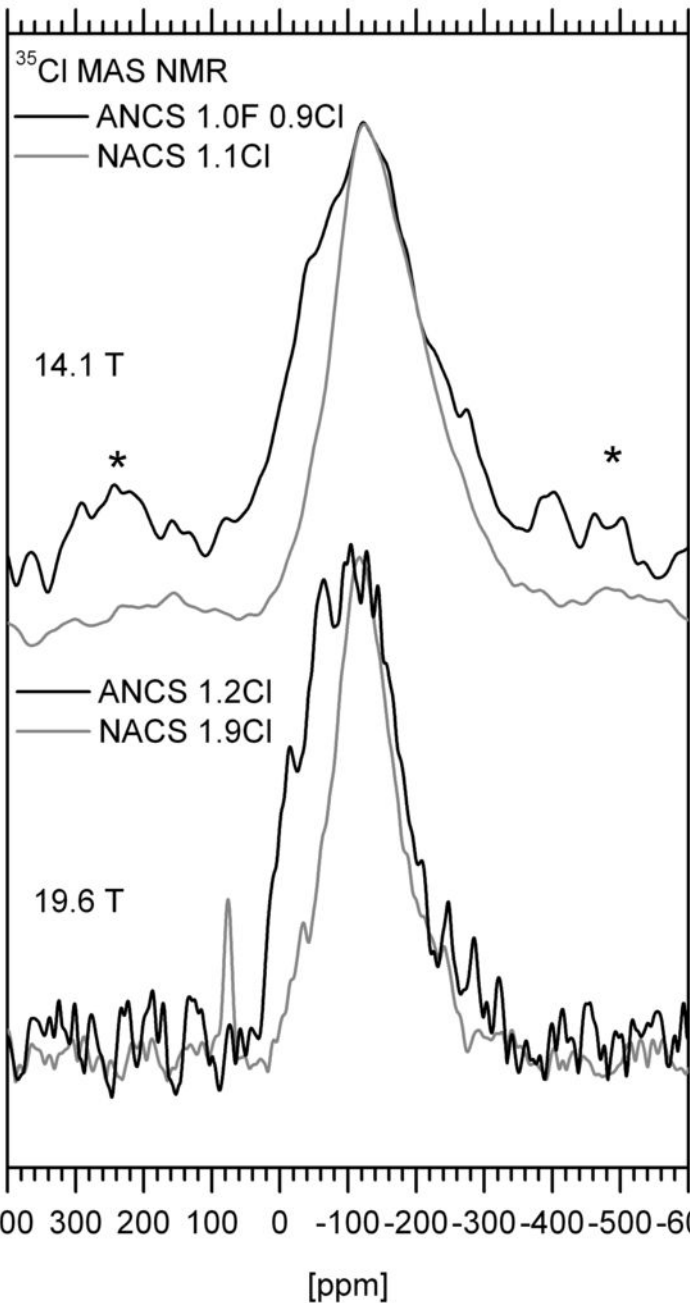
— ANCS 1.2Cl

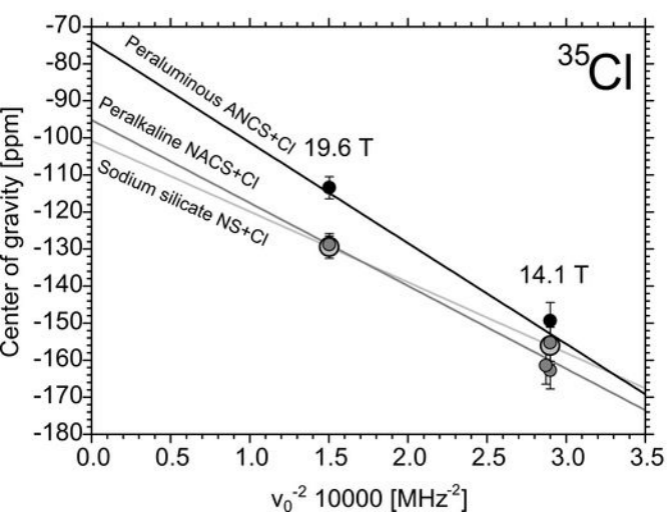
— NACS 1.9Cl

19.6 T

400 300 200 100 0 -100 -200 -300 -400 -500 -600

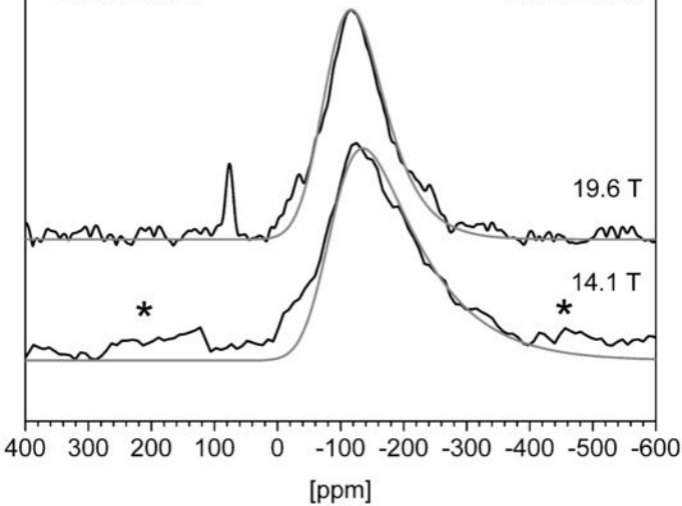
[ppm]

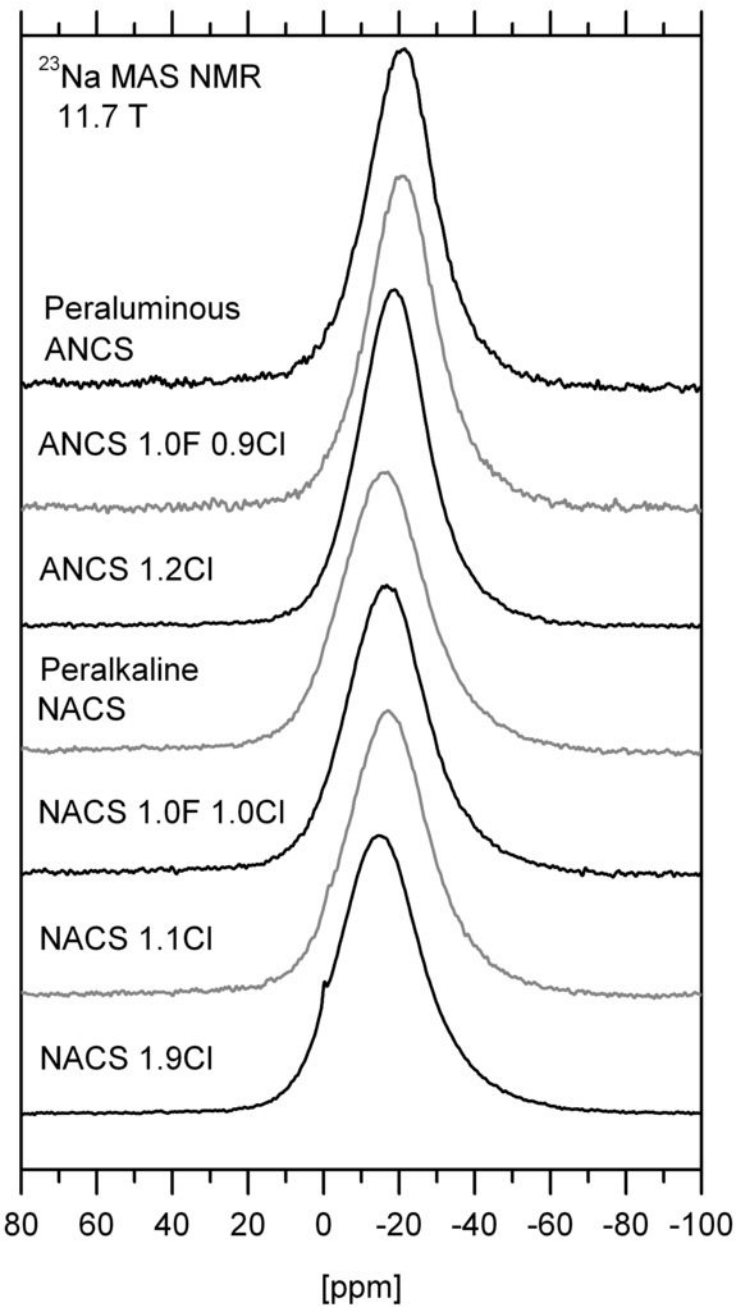




^{35}Cl MAS NMR

NACS 1.1Cl

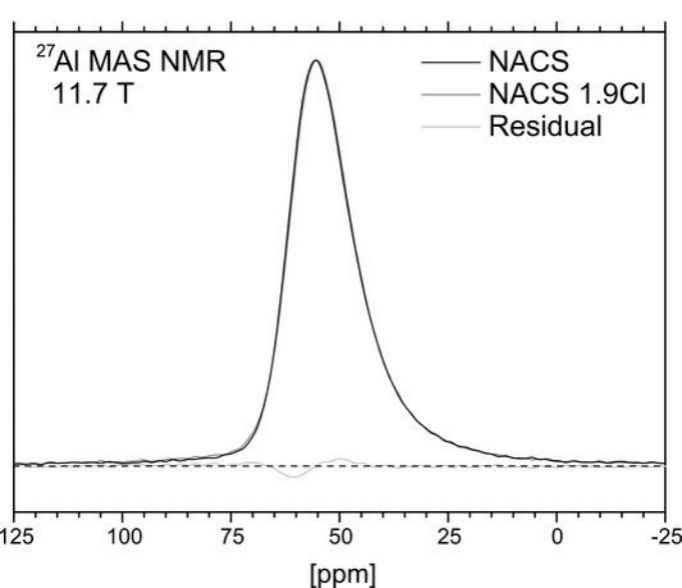




^{27}Al MAS NMR
11.7 T

— NACS
— NACS 1.9Cl
— Residual

125 100 75 50 25 0 -25
[ppm]



^{27}Al MAS NMR
20 T

— ANCS
— ANCS 1.2Cl
— Residual

